JEM Journal of Experimental Medicine

ARTICLE

Retinoic acid signaling during priming licenses intestinal CD103+ CD8 T_{RM} cell differentiation

Zhijuan Qiu[1], Camille Khairallah[1], Timothy H. Chu[1], Jessica N. Imperato[1], Xinyuan Lei[1], Galina Romanov[1], Amha Atakilit[2], Lynn Puddington[3], and Brian S. Sheridan[1]

CD8 tissue-resident memory T (T_{RM}) cells provide frontline protection at barrier tissues; however, mechanisms regulating T_{RM} cell development are not completely understood. Priming dictates the migration of effector T cells to the tissue, while factors in the tissue induce in situ T_{RM} cell differentiation. Whether priming also regulates in situ T_{RM} cell differentiation uncoupled from migration is unclear. Here, we demonstrate that T cell priming in the mesenteric lymph nodes (MLN) regulates CD103+ T_{RM} cell differentiation in the intestine. In contrast, T cells primed in the spleen were impaired in the ability to differentiate into CD103+ T_{RM} cells after entry into the intestine. MLN priming initiated a CD103+ T_{RM} cell gene signature and licensed rapid CD103+ T_{RM} cell differentiation in response to factors in the intestine. Licensing was regulated by retinoic acid signaling and primarily driven by factors other than CCR9 expression and CCR9-mediated gut homing. Thus, the MLN is specialized to promote intestinal CD103+ CD8 T_{RM} cell development by licensing in situ differentiation.

Introduction

Memory CD8 T cells can be divided into three populations based on their migratory patterns: circulating central and effector memory T cells and tissue-resident memory T (T_{RM}) cells (Gebhardt et al., 2009; Masopust et al., 2010; Mueller and Mackay, 2016; Park and Kupper, 2015; Sallusto et al., 1999; Sheridan and Lefrançois, 2011). T_{RM} cells primarily reside in non-lymphoid tissues and are phenotypically, functionally, transcriptionally, and metabolically distinct from circulating memory T cell subsets (Kumar et al., 2017; Mackay et al., 2016; Mackay et al., 2013; Masopust et al., 2006; Pan et al., 2017; Wakim et al., 2012). CD8 T_{RM} cells predominately express CD69, and the majority of those that reside within epithelium also express the α_E integrin, CD103. CD69 promotes the residency of CD8 T_{RM} cells in non-lymphoid tissues by inhibiting sphingosine-1-phosphate receptor-mediated egress of CD8 T_{RM} cells from non-lymphoid tissues (Bankovich et al., 2010; Mackay et al., 2015; Shiow et al., 2006; Skon et al., 2013). CD103 binds to E-cadherin expressed in adherens junctions of epithelial cells and plays an important role in the accumulation and retention of CD8 T_{RM} cells in barrier tissues (Casey et al., 2012; Lee et al., 2011; Mackay et al., 2013; Sheridan et al., 2014). CD8 T_{RM} cells play a critical role in protective immunity against infections and cancer (Ganesan et al., 2017; Gebhardt et al., 2009; Jiang et al., 2012; Malik et al., 2017; Nizard et al., 2017; Sheridan et al., 2014; Shin and Iwasaki, 2012; Wu et al., 2014). They are prepositioned in the tissue to respond immediately to pathogen re-encounter and mediate protective immunity through multiple mechanisms like direct lysis of infected cells, induction of broadly active antimicrobial genes, or by activating innate immune cells and recruiting circulating memory cells through the release of cytokines IFNγ, IL-2, and TNFα (Ariotti et al., 2014; Cheuk et al., 2017; Schenkel et al., 2014; Schenkel et al., 2013). Thus, it is important to understand the mechanisms regulating the development and maintenance of CD8 T_{RM} cells in specific tissues.

The development of CD8 T_{RM} cells involves several steps including T cell priming in draining lymphoid organs, T cell migration to non-lymphoid tissues, and in situ T_{RM} cell differentiation mediated by environmental signals. Priming in specific lymphoid organs instructs the migration of effector CD8 T cells to appropriate tissues, providing a critical point of regulation for the induction of proper tissue T cell responses (Park and Kupper, 2015; Sheridan and Lefrançois, 2011). Inherent factors in the tissue environment are essential for in situ CD8 T_{RM} cell differentiation (Masopust et al., 2006). TGFβ activated by α_v integrins on stromal cells in the tissue environment is crucial for inducing CD103 expression on CD8 T_{RM} cells (Casey et al., 2012;

[1]Department of Microbiology and Immunology, Center for Infectious Diseases, Renaissance School of Medicine, Stony Brook University, Stony Brook, NY, USA; [2]Lung Biology Center, Department of Medicine, University of California, San Francisco, San Francisco, CA, USA; [3]Department of Immunology, University of Connecticut Health, Farmington, CT, USA.

Correspondence to Brian S. Sheridan: brian.sheridan@stonybrook.edu.

Lee et al., 2011; Mackay et al., 2013; Mohammed et al., 2016; Qiu et al., 2021; Sheridan et al., 2014; Zhang and Bevan, 2013). Local extrinsic factors such as pathogen-induced inflammation and cognate antigen can have additional impacts on CD103$^+$ CD8 T_{RM} cell differentiation, although the findings are often dictated by the environment these cells reside in and the pathogen or infection route utilized (Bergsbaken and Bevan, 2015; Bergsbaken et al., 2017; Casey et al., 2012; Khan et al., 2016; Kohlmeier et al., 2007; Lee et al., 2011; Mackay et al., 2012; Muschaweckh et al., 2016; Slutter et al., 2017; Wakim et al., 2010). While the impact of local environment on CD103$^+$ CD8 T_{RM} cell differentiation has been extensively studied, whether CD8 T cell priming in draining lymphoid organs regulates in situ CD103$^+$ T_{RM} cell differentiation has not been established. The site of T cell priming is determined by the route of immunization. As the route of immunization is a critical factor in vaccine development, understanding the role of T cell priming in regulating CD103$^+$ CD8 T_{RM} cell differentiation will provide important insights into CD8 T_{RM} cell biology that can be applied to improving vaccine strategies.

While priming in the mesenteric lymph nodes (MLN) has long been known to promote T cell homing to gut tissues, we report an additional distinct mechanism by which priming in the MLN promotes intestinal CD8 T_{RM} cell formation. Priming in the MLN licensed CD8 T cells to respond to factors in the intestine to differentiate into CD103$^+$ T_{RM} cells. In contrast, CD8 T cells primed in the spleen were remarkably inefficient at differentiating into CD103$^+$ T_{RM} cells after migration into gut tissues. Moreover, priming in the MLN, rather than preconditioning during homeostasis, was the major determinant of in situ CD103$^+$ CD8 T_{RM} cell differentiation after migration into the intestine. We further demonstrate that MLN priming initiated CD103$^+$ T_{RM} cell gene signature before emigration out of the MLN, and retinoic acid (RA) signaling provided during priming licensed intestinal CD103$^+$ T_{RM} cell differentiation. While CCR9 contributed to CD103$^+$ CD8 T_{RM} cell development, the impact of RA signaling on licensing CD103$^+$ CD8 T_{RM} cell development appears primarily driven by factors other than CCR9 induction and gut homing. Therefore, our study establishes a distinct property of MLN priming to license CD103$^+$ CD8 T_{RM} cell development in the intestine.

Results

Priming in the MLN promotes CD103$^+$ CD8 T_{RM} precursor cell differentiation in the intestine

To study the impact of priming on intestinal CD103$^+$ CD8 T_{RM} cell differentiation, we first utilized an i.v. vs. foodborne infection model with a murinized recombinant *Listeria monocytogenes* strain containing a mutation in the internalin A protein (InlA^M r*Lm*) that allows efficient invasion of the murine intestinal epithelium (Wollert et al., 2007). One of the major differences between i.v. and foodborne *L. monocytogenes* infection is the priming site for T cells (Qiu et al., 2018). While it is well documented that the spleen is the primary priming site after i.v. *L. monocytogenes* infection (Khanna et al., 2007), the MLN is the draining lymph node and a major priming site after foodborne *L. monocytogenes* infection (Imperato et al., 2020). We employed a two-step adoptive transfer system to assess CD8 T cells primed in distinct lymphoid organs (Fig. 1 A). 1×10^4 naive OT-I cells (which express a transgenic T cell receptor that recognizes $OVA_{257-264}$ presented in H2-K^b) were isolated from the spleen of OT-I *Rag1*$^{-/-}$ mice and transferred into congenic mice 1 d prior to infection. Mice were i.v. or foodborne infected with InlA^M *Lm* expressing OVA (InlA^M *Lm*-OVA). At 5.5 d postinfection (dpi), effector OT-I cells were isolated from the spleen of i.v.-infected mice (spleen-primed T cells) or the MLN of foodborne-infected mice (MLN-primed T cells) by FACS sorting based on congenic marker expression. 5×10^5 sorted effector OT-I cells were transferred into congenic recipient mice that were foodborne InlA^M *Lm*-OVA infected 5.5 d previously, providing similar intestinal environments for effector cells primed at distinct lymphoid organs. 1 and 3 d after transfer, donor OT-I cells in recipient mice were analyzed. Priming in specific lymphoid organs dictates the migratory pattern of effector CD8 T cells (Park and Kupper, 2015; Sheridan and Lefrançois, 2011). In this manner, as previously reported (Johansson-Lindbom et al., 2003), priming in the MLN instructed CD8 T cells to express $\alpha_4\beta_7$ and CCR9 (Fig. 1 B). CD8 T cells primed in the spleen also expressed $\alpha_4\beta_7$, but to a significantly lesser extent (Fig. 1 B). Moreover, they failed to express CCR9 (Fig. 1 B). Consistent with previous studies (Masopust et al., 2010), MLN-primed T cells preferentially migrated to the lamina propria (LP) and intraepithelial lymphocytes (IEL) compartment compared with spleen-primed T cells (Fig. 1 C). These data demonstrate that priming in the MLN induced greater $\alpha_4\beta_7$ and CCR9 expression on CD8 T cells and promoted their migration to the intestine.

Our previous study demonstrated that foodborne InlA^M *Lm* infection induces rapid differentiation of CD103$^+$ CD8 T_{RM} precursor cells in the intestine (Sheridan et al., 2014). We next examined whether priming regulated this rapid CD103$^+$ CD8 T_{RM} precursor cell differentiation. 1 d after transfer, MLN-primed T cells that migrated into the intestine started to upregulate CD69 and CD103 co-expression, while spleen-primed T cells failed to coupregulate CD69 and CD103 (Fig. 1 D). Donor cells did not express CD69 or CD103 prior to transfer (Fig. S1 A), suggesting that entry into the intestines led to upregulation of CD69 and CD103 on MLN-primed but not spleen-primed CD8 T cells. 3 d after transfer, MLN-primed T cells in the LP and IEL compartment had efficiently differentiated into CD103$^+$ T_{RM} precursor cells (Fig. 1 E). In comparison, spleen-primed cells failed to differentiate into CD103$^+$ T_{RM} precursor cells in either tissue (Fig. 1 E). Additionally, MLN-primed T cells that migrated to the spleen did not differentiate into CD103$^+$ T_{RM} precursor cells (Fig. 1 E), suggesting that factors existing in the intestine were critical for CD103$^+$ T_{RM} precursor cell differentiation.

Similar results were observed when spleen-primed and MLN-primed T cells were transferred into naive congenic recipient mice (Fig. 1, F–H), suggesting basal intestinal inherent factors alone were sufficient to drive MLN-primed but not spleen-primed T cells to rapidly differentiate into CD103$^+$ T_{RM} precursor cells. Thus, our data demonstrate that MLN, but not splenic priming, promotes CD8 T cell responsiveness to environmental signals present in the small intestine for CD103$^+$ T_{RM} precursor cell differentiation.

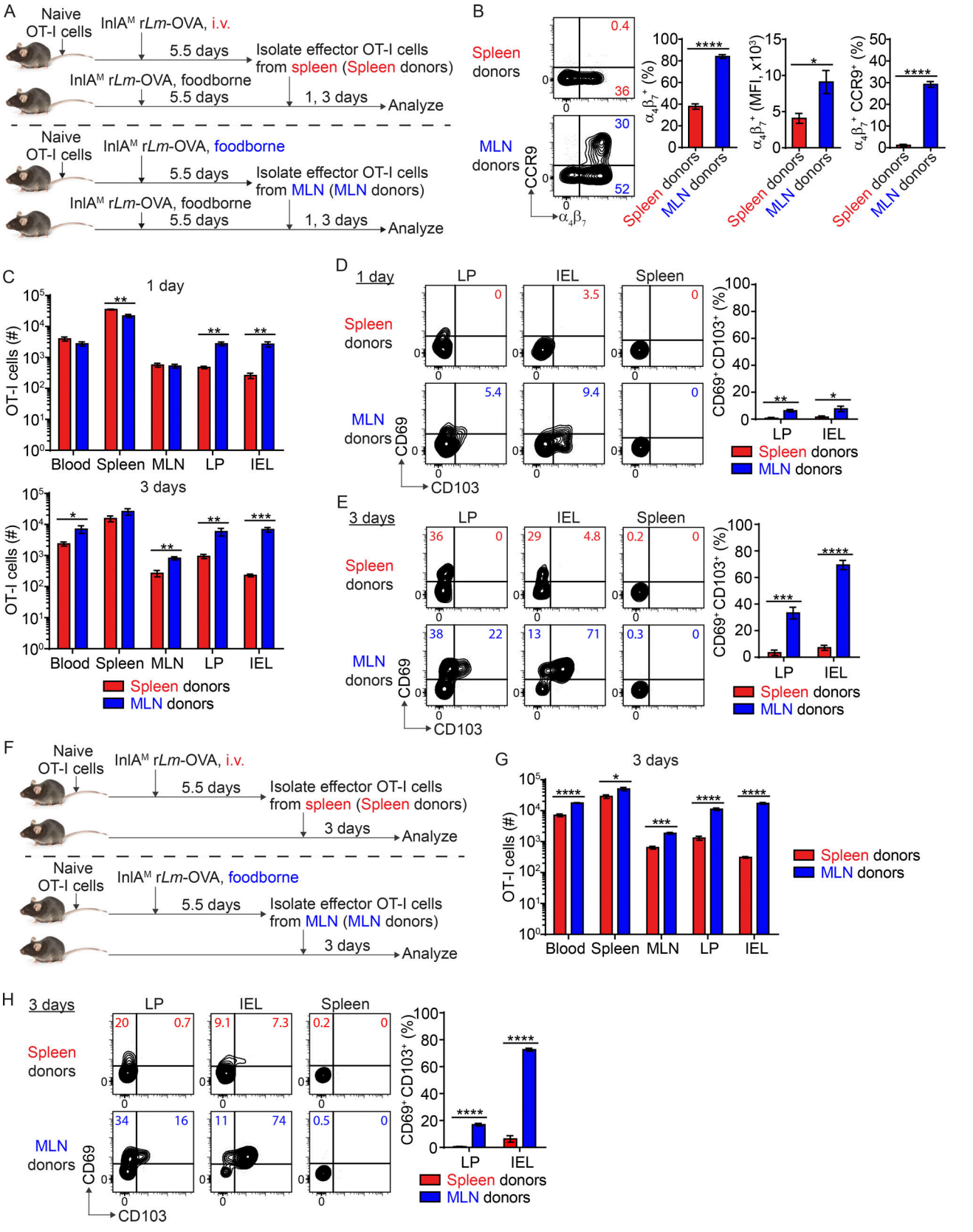

Figure 1. **Priming in the MLN promotes CD103⁺ CD8 T_{RM} precursor cell differentiation in the intestine. (A)** Experimental design for B–E. 1 × 10^4 naive OT-I cells were transferred into congenic naive first recipient mice. 1 d later, mice were i.v. or foodborne infected with InlA^M *Lm*-OVA. At 5.5 dpi, effector OT-I cells were isolated from the spleen of i.v.-infected mice (spleen donors) or the MLN of foodborne-infected mice (MLN donors) by FACS sorting based on congenic marker expression. 5 × 10^5 sorted effector OT-I cells were transferred into congenic second recipient mice that were foodborne InlA^M *Lm*-OVA

infected 5.5 d previously. 1 and 3 d after transfer, donor OT-I cells in the second recipient mice were analyzed. **(B)** The expression of $\alpha_4\beta_7$ and CCR9 by effector OT-I cells prior to adoptive transfer into the second recipient mice. **(C)** Numbers of donor OT-I cells in indicated tissues at 1 and 3 d after transfer. **(D)** The expression of CD69 and CD103 by donor OT-I cells in the LP and IEL compartment at 1 d after transfer. **(E)** The expression of CD69 and CD103 by donor OT-I cells in the LP and IEL compartment at 3 d after transfer. **(F)** Experimental design for G and H. 1×10^4 naive OT-I cells were transferred into congenic naive first recipient mice 1 d prior to i.v. or foodborne infection with $InlA^M$ *Lm*-OVA. At 5.5 dpi, 5×10^5 spleen donors or MLN donors were sorted and transferred into congenic naive second recipient mice. 3 d after transfer, donor OT-I cells in the second recipient mice were analyzed. **(G)** Numbers of donor OT-I cells in indicated tissues at 3 d after transfer. **(H)** The expression of CD69 and CD103 by donor OT-I cells in the LP and IEL compartment at 3 d after transfer. The data in B are pooled from five independent experiments, $n = 5$ experiments. For each experiment, 2–18 mice were pooled for spleen donors and 18–34 mice were pooled for MLN donors. The data in C–E and G–H are representative of three independent experiments, $n = 4$–5 mice/experiment. The data are expressed as mean ± SEM. Unpaired *t* tests were performed (B–D, G, and H). *, $P \le 0.05$; **, $P \le 0.01$; ***, $P \le 0.001$; ****, $P \le 0.0001$.

We next examined whether priming regulated CD103$^-$ T_{RM} precursor cell differentiation. Regardless of whether effector T cells were transferred into previously infected recipient mice or naive mice, while MLN-primed T cells were slightly more efficient at differentiating into CD103$^-$ T_{RM} precursor cells in the LP, they were less efficient at differentiating into CD103$^-$ T_{RM} precursor cells in the IEL compartment (Fig. S1, B and C). Overall, the impact of priming on CD103$^-$ T_{RM} precursor cell differentiation is less substantial and appeared compartmentalized.

To determine whether the intrinsic environment of the MLN had an impact on CD103$^+$ T_{RM} precursor cell differentiation, effector T cells were sorted from the spleen and MLN of i.v.-infected mice or from the spleen and MLN of foodborne-infected mice and transferred into naive congenic recipient mice for analysis 3 d later (Fig. S1 D). Since CD8 T cells are primed in the MLN but not spleen after foodborne infection (Imperato et al., 2020; Sheridan et al., 2014), effector T cells isolated from the spleen after foodborne infection are likely migrants. Additionally, *L. monocytogenes* did not invade the gut or MLN after i.v. infection (Fig. S1 E), suggesting that effector T cells isolated from the MLN after i.v. infection are not primed there but are migrants. Compared to foodborne MLN donor cells, foodborne spleen donor cells had reduced $\alpha_4\beta_7$ and CCR9 expression (Fig. S1 F). Compared with i.v. spleen donors, i.v. MLN donors had higher $\alpha_4\beta_7$ and CCR9 expression, suggesting the MLN environment enhanced gut-homing receptor expression on migrant effector T cells (Fig. S1 F). Foodborne spleen donors lost some ability to differentiate into CD103$^+$ T_{RM} precursor cells in the intestine compared to foodborne MLN donors (Fig. S1 G). Surprisingly, i.v. MLN donors gained the ability to differentiate into intestinal CD103$^+$ T_{RM} precursor cells compare to i.v. spleen donors, albeit to a lesser degree than foodborne MLN donors (Fig. S1 G). Thus, the MLN imparts an environment signal in addition to priming that promotes effector CD8 T cell differentiation into CD103$^+$ T_{RM} precursor cells in the intestine.

Rapid intestinal CD103$^+$ CD8 T_{RM} precursor cell differentiation is independent of activation stage, intestinal homing, and KLRG-1 expression

While i.v. and foodborne *L. monocytogenes* infection induced a similar magnitude of circulating OVA-specific CD8 T cells, the initiation and peak of the CD8 T cell response were delayed by 1 d after foodborne infection (Fig. S2 A). We sought to determine whether the difference in intestinal CD103$^+$ T_{RM} precursor cell differentiation between spleen-primed and MLN-primed T cells was due to a difference in activation stages at the time of transfer. To address this, effector OT-I cells were isolated from the spleen at 4.5 d after i.v. infection and from the MLN at 5.5 d after foodborne infection for adoptive transfer into mice that were foodborne-infected 5.5 d previously (Fig. S2 B), putting spleen-primed and MLN-primed T cells at a comparable activation stage based on the time to peak response. 4.5-d spleen-primed T cells did not express CCR9; however, they expressed a higher frequency of $\alpha_4\beta_7$ (Fig. S2 C and Fig. 1 B) and accumulated in the LP as efficiently as 5.5-d MLN-primed T cells (Fig. S2 D), suggesting that splenic priming was as capable of inducing LP-migrant T cells as MLN priming. However, rescued LP migration did not restore the migration to the IEL compartment (Fig. S2 D), consistent with a role for CCR9 in mediating the accumulation of antigen-specific T cells in the epithelium (Johansson-Lindbom et al., 2003). Regardless, 4.5-d spleen-primed T cells failed to rapidly differentiate into CD103$^+$ T_{RM} precursor cells after migration into the LP or IEL compartment (Fig. S2 E), indicating that spleen-primed CD8 T cells have an inherent and limited capacity to differentiate into CD103$^+$ T_{RM} precursor cells in the intestinal LP that is independent of activation stage and intestinal homing ability. To confirm that the inability of spleen-primed T cells to differentiate into CD103$^+$ T_{RM} precursor cells was independent of their ability to accumulate in the intestine, eight times more spleen-primed T cells were transferred into recipient mice (Fig. S2 F). Although a greater number of spleen-primed T cells accumulated in the LP and IEL compartments with an increased number of transferred cells (Fig. S2 G), spleen-primed T cells remained largely unable to differentiate into CD103$^+$ T_{RM} precursor cells (Fig. S2 H). Thus, inability of spleen-primed T cells to differentiate into CD103$^+$ T_{RM} precursor cells was independent of their intestinal homing and accumulation.

Previous studies have demonstrated that CD103$^+$ CD8 T_{RM} cells are derived from KLRG-1$^-$ cells (Mackay et al., 2013; Sheridan et al., 2014). It is plausible that priming in the MLN may promote KLRG-1$^-$ cells. Indeed, 5.5-d MLN-primed T cells had a slightly but significantly higher percentage of KLRG-1$^-$ cells than 5.5-d spleen-primed T cells (Fig. S2 I); however, they had a slightly but significantly lower percentage of KLRG-1$^-$ cells than 4.5-d spleen-primed T cells (Fig. S2 J). As both 4.5- and 5.5-d spleen-primed T cells failed to rapidly differentiate into CD103$^+$ T_{RM} precursor cells (Fig. S2 E and Fig. 1 E), the inability of spleen-primed CD8 T cells to differentiate into CD103$^+$ T_{RM} precursor cells did not correlate with the proportion of KLRG-1$^-$ cells among donor cells. To further confirm that the proportion of KLRG-1$^-$cells did not impact CD103$^+$ T_{RM} precursor cell differentiation, KLRG-1$^-$ effector cells were isolated from the

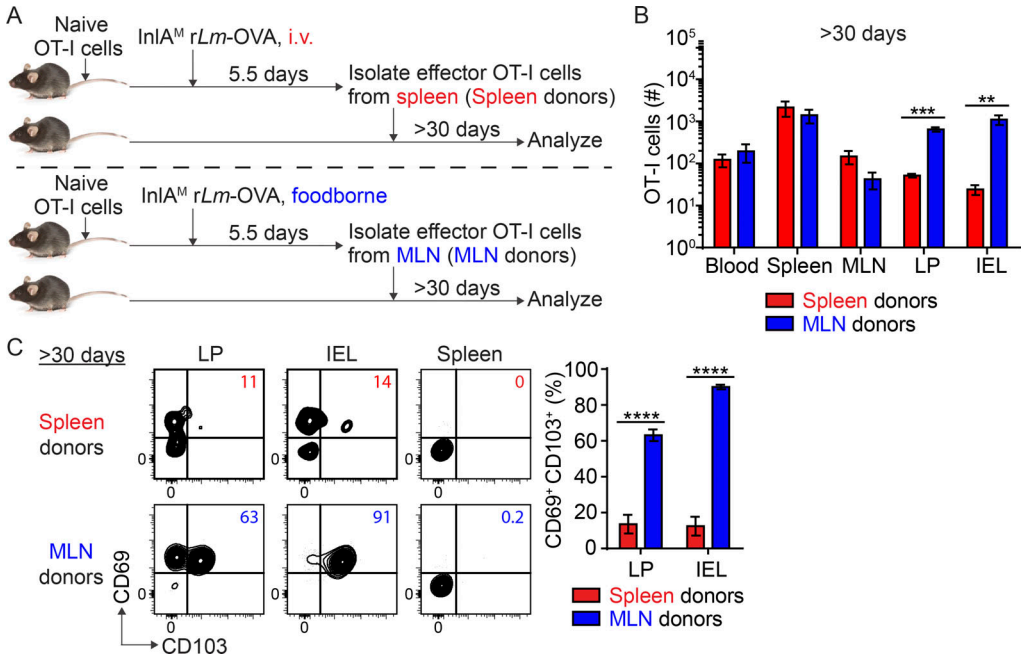

Figure 2. **Priming in the MLN licenses intestinal CD103⁺ CD8 T_{RM} cell differentiation. (A)** Experimental design. 1 × 10^4 naive OT-I cells were transferred into congenic naive first recipient mice 1 d prior to i.v. or foodborne infection with $InlA^M$ *Lm*-OVA. At 5.5 dpi, 5 × 10^5 spleen donors or MLN donors were sorted and transferred into congenic naive second recipient mice. >30 d after transfer, donor OT-I cells in the second recipient mice were analyzed. **(B)** Numbers of donor OT-I cells in indicated tissues at >30 d after transfer. **(C)** The expression of CD69 and CD103 by donor OT-I cells in the LP and IEL compartment at >30 d after transfer. The data in B and C are representative of two independent experiments, *n* = 4 mice/experiment. The data are expressed as mean ± SEM. Unpaired *t* tests were performed (B and C). **, P ≤ 0.01; ***, P ≤ 0.001; ****, P ≤ 0.0001.

spleen at 4.5 d after i.v. infection and from the MLN at 5.5 d after foodborne infection for adoptive transfer into naive mice (Fig. S2 K). While 4.5-d KLRG-1⁻ spleen-primed T cells accumulated in the LP as efficiently as 5.5-d KLRG-1⁻ MLN-primed T cells (Fig. S2 L), they failed to rapidly differentiate into CD103⁺ T_{RM} precursor cells after migration into the LP and IEL compartments (Fig. S2 M). These data are consistent with the notion that rapid CD103⁺ T_{RM} precursor cell differentiation is independent of KLRG-1 expression.

Priming in the MLN licenses intestinal CD103⁺ CD8 T_{RM} cell development

As MLN priming promoted rapid in situ CD103⁺ T_{RM} precursor cell differentiation, we next evaluated its impact on CD103⁺ T_{RM} cell development at memory. The basal intestinal environment was sufficient to support CD103⁺ T_{RM} precursor cell differentiation (Fig. 1 H and Fig. S3, A and B), and more effector CD8 T cells could be recovered from a naive host than an infected host (Fig. S3 C), enhancing our ability to detect transferred cells at memory. As such, spleen-primed and MLN-primed CD8 T cells were adoptively transferred into naïve mice to assess their capacity to become CD103⁺ T_{RM} cells (Fig. 2 A). At >30 d after transfer, spleen-primed and MLN-primed CD8 T cells were detected in all tissues examined, but significantly more MLN-primed T cells were present in the LP and IEL compartments (Fig. 2 B), suggesting MLN priming led to a significantly larger memory CD8 T cell pool in the intestine. Consistent with the enhanced CD103⁺ T_{RM} precursor cell differentiation among MLN-primed cells, the majority of MLN-primed T cells in the LP and IEL compartments became CD103⁺ T_{RM} cells (Fig. 2 C). In stark contrast, spleen-primed T cells remained largely incapable of differentiating into CD103⁺ T_{RM} cells after 30 d (Fig. 2 C). Importantly, most spleen-primed T cells acquired a CD127⁺ KLRG-1⁻ memory phenotype in the intestine at this time (Fig. S3 D), suggesting that they are capable of becoming cells with a memory phenotype but not upregulating CD103. Consistent with transfer into naive mice, spleen-primed T cells were inefficient at CD103⁺ T_{RM} cell differentiation after adoptive transfer into previously infected mice (Fig. S3 F), suggesting that the local environment is insufficient to induce CD8 T_{RM} cell differentiation in the absence of appropriate licensing. Altogether, these data demonstrated that priming in the MLN licensed CD103⁺ T_{RM} cell development in the intestine.

While spleen-primed T cells were not efficient at differentiating into CD103⁺ T_{RM} cells, they were readily detectable in the intestine at memory. We next determined whether these memory cells were resident cells or a transient migratory population. Spleen-primed T cells were adoptively transferred into naive mice (Fig. S3 G). 6 d later, after these effector cells had completely downregulated $\alpha_4\beta_7$ expression, recipient mice were treated with vehicle control or FTY720 daily for 3 wk to block tissue egress of T cells (Hirai et al., 2019). The numbers of CD69⁻ CD103⁻ cells in the LP and IEL compartments were significantly increased in FTY720-treated mice compared to vehicle-treated mice, while the numbers of CD69⁺ CD103⁻ and CD69⁺ CD103⁺ cells were largely comparable between these two groups (Fig. S3 H). These data suggest that while CD69⁺ populations are likely resident cells, CD69⁻ CD103⁻ cells represent a transient

migratory population, which is consistent with previous studies (Hirai et al., 2019; Mackay et al., 2015; Takamura et al., 2016).

Priming, but not preconditioning, promotes rapid CD103$^+$ T_{RM} cell differentiation in the intestine

A recent study demonstrated that migratory dendritic cells (DCs) activate TGFβ through α_V integrins and present it to naive CD8 T cells in lymph nodes to precondition them for CD103$^+$ T_{RM} cell differentiation in the skin (Mani et al., 2019). We set to determine the respective contribution of preconditioning versus priming to the differentiation of CD103$^+$ T_{RM} cells in the intestine. CD103 expression on naive T cells indicates TGFβ-mediated preconditioning occurred in lymph nodes (Mani et al., 2019). As such, CD103$^+$ and CD103$^-$ naïve OT-I cells were sorted from the spleen of OT-I *Rag1*$^{-/-}$ mice and transferred into naive congenic mice (Fig. 3 A and Fig. S4 A). Recipient mice were i.v.- or foodborne-infected with InlA^M *Lm*-OVA 1 d after transfer. At 5.5 dpi, effector OT-I cells were sorted from the spleen of i.v.-infected mice or the MLN of foodborne-infected mice and transferred into naive congenic recipient mice. Of note, CD103$^+$ naive OT-I cells completely downregulated CD103 expression after activation (Fig. S4 B). 3 d after transfer, CD103 status of naive T cells did not significantly affect the accumulation of either spleen-primed or MLN-primed T cells in the intestine (Fig. 3 B). Interestingly, regardless of whether donor CD8 T cells were preconditioned (CD103$^+$) or not (CD103$^-$), as long as they were primed in the MLN, they were equally efficient in differentiating into CD103$^+$ T_{RM} precursor cells in the intestine (Fig. 3 C). Thus, priming, but not preconditioning, appears to be the major determinant of rapid CD103$^+$ T_{RM} precursor cell differentiation in the intestine. While CD103 expression depends on TGF-β signaling and is used as a surrogate marker of TGFβ-mediated preconditioning (Mani et al., 2019; Zhang and Bevan, 2012), it does not preclude that CD103$^-$ naive T cells are not preconditioned by TGF-β. Since TGF-β activation and TGFβ-mediated preconditioning in lymph nodes rely on $\alpha_v\beta_8$ expressed by migratory DCs (Mani et al., 2019; Qiu et al., 2021), anti-$\alpha_v\beta_8$ was used to block TGF-β activation and TGFβ-mediated preconditioning. Naive OT-I *Rag1*$^{-/-}$ mice were treated with PBS or anti-$\alpha_v\beta_8$ weekly for 3 wk (Dodagatta-Marri et al., 2021; Hirai et al., 2021; Fig. 3 D). Anti-$\alpha_v\beta_8$ treatment led to a 50% reduction in CD103 expression in naive T cells (Fig. 3 E). Naive OT-I cells were then isolated and transferred into congenic mice 1 d prior to infection. At 5.5 dpi, effector OT-I cells were sorted from the spleen of i.v.-infected mice or the MLN of foodborne-infected mice and transferred into naive congenic recipient mice. Anti-$\alpha_v\beta_8$ treated and untreated effector T cells accumulated similarly in the intestine of recipient mice 3 d after transfer (Fig. 3 F). More importantly, they both efficiently differentiated into intestinal CD103$^+$ T_{RM} precursor cells (Fig. 3 G) and CD103$^+$ T_{RM} cells (Fig. 3 H), if they were primed in the MLN. These results are consistent with the notion that priming, but not preconditioning, promotes CD103$^+$ T_{RM} cell differentiation in the intestine.

A CD103$^+$ T_{RM} cell gene signature is initiated prior to emigration from the MLN

We next attempted to determine how priming regulated intestinal CD103$^+$ T_{RM} cell differentiation. Naive, spleen-primed, and MLN-primed OT-I cells were isolated and sequenced for transcriptional profiling (Fig. 4 A). Principle component analysis showed that the transcription profile was distinct between MLN-primed and spleen-primed T cells (Fig. 4 B). Based on the criteria for significance ($P \le 0.05$ and fold change ≥2), 158 genes were differentially expressed, of which 52 genes were upregulated and 106 genes were downregulated in MLN-primed T cells compared with spleen-primed T cells (Fig. 4 C and Table. S1). Of the top 10 most upregulated genes in the MLN-primed T cells, two were associated with the core CD103$^+$ CD8 T_{RM} cell signature (*Itgae* and *Xcl1*) and four were associated with the gut CD103$^+$ CD8 T_{RM} cell signature (*Ccr9*, *Itgae*, *Xcl1*, and *P2rx7*; Fig. 4 D; Mackay et al., 2013). Moreover, T cell-intrinsic expression of *Hic 1* has been shown to promote CD103$^+$ resident LP lymphocytes and IEL during homeostasis (Burrows et al., 2017). A recent study further identified *Hic1* as a critical regulator of T_{RM} cell differentiation in the IEL compartment (Crowl et al., 2022). Since gene expression profile changes temporally during T cell activation (Best et al., 2013), and 5.5-d spleen-primed T cells and 5.5-d MLN-primed T cells were likely at different activation stages (Fig. S2 A), we determined whether differentially expressed genes resulted from distinct priming environments or a difference in their activation stage. Quantitative PCR was performed using both 4.5- and 5.5-d spleen-primed T cells in comparison with 5.5-d MLN-primed T cells. 7 out of the 10 indicated genes (*Ccr9*, *Hic1*, *Car2*, *Itgae*, *Lztfl1*, *Xcl1*, and *P2rx7*) had at least twofold higher expression in 5.5-d MLN-primed T cells compared with both 4.5- and 5.5-d spleen-primed T cells (Fig. 4 E). Overall, these data suggest that MLN priming initiated a CD103$^+$ CD8 T_{RM} cell gene signature before effector CD8 T cells emigrated from the MLN.

CCR9 expression contributes to intestinal CD103$^+$ T_{RM} cell differentiation

Itgae, which encodes CD103, was one of the most upregulated genes in MLN-primed T cells compared with spleen-primed T cells (Fig. 4, D and E). We next examined whether this reduced *Itgae* gene expression in spleen-primed T cells contributed to their inability to upregulate CD103 protein expression in response to TGF-β. 4.5- and 5.5-d spleen-primed T cells and 5.5-d MLN-primed T cells were cultured with TGF-β in vitro for 24 h followed by flow analysis of CD103 protein expression (Fig. S4 C). While 5.5-d spleen-primed T cells had impaired ability to upregulate CD103 protein expression, 4.5-d spleen-primed T cells were equally efficient as 5.5 d MLN-primed T cells to upregulate CD103 protein expression in response to TGF-β in vitro (Fig. S4 D). Nevertheless, neither 4.5-d spleen-primed T cells nor 5.5-d spleen-primed T cells were able to differentiate into CD103$^+$ T_{RM} precursor cells in vivo (Fig. 1 E and Fig. S2 E). These data collectively suggest that reduced *Itgae* gene expression was not a major contributor to the inability of spleen-primed CD8 T cells to differentiate into CD103$^+$ T_{RM} precursor cells in the intestine.

Ccr9 was the most upregulated gene in MLN-primed T cells compared with spleen-primed T cells (Fig. 4, D and E). A previous study demonstrated that CCR9 promotes the induction of CD103 expression on CD8 T cells following their entry into the

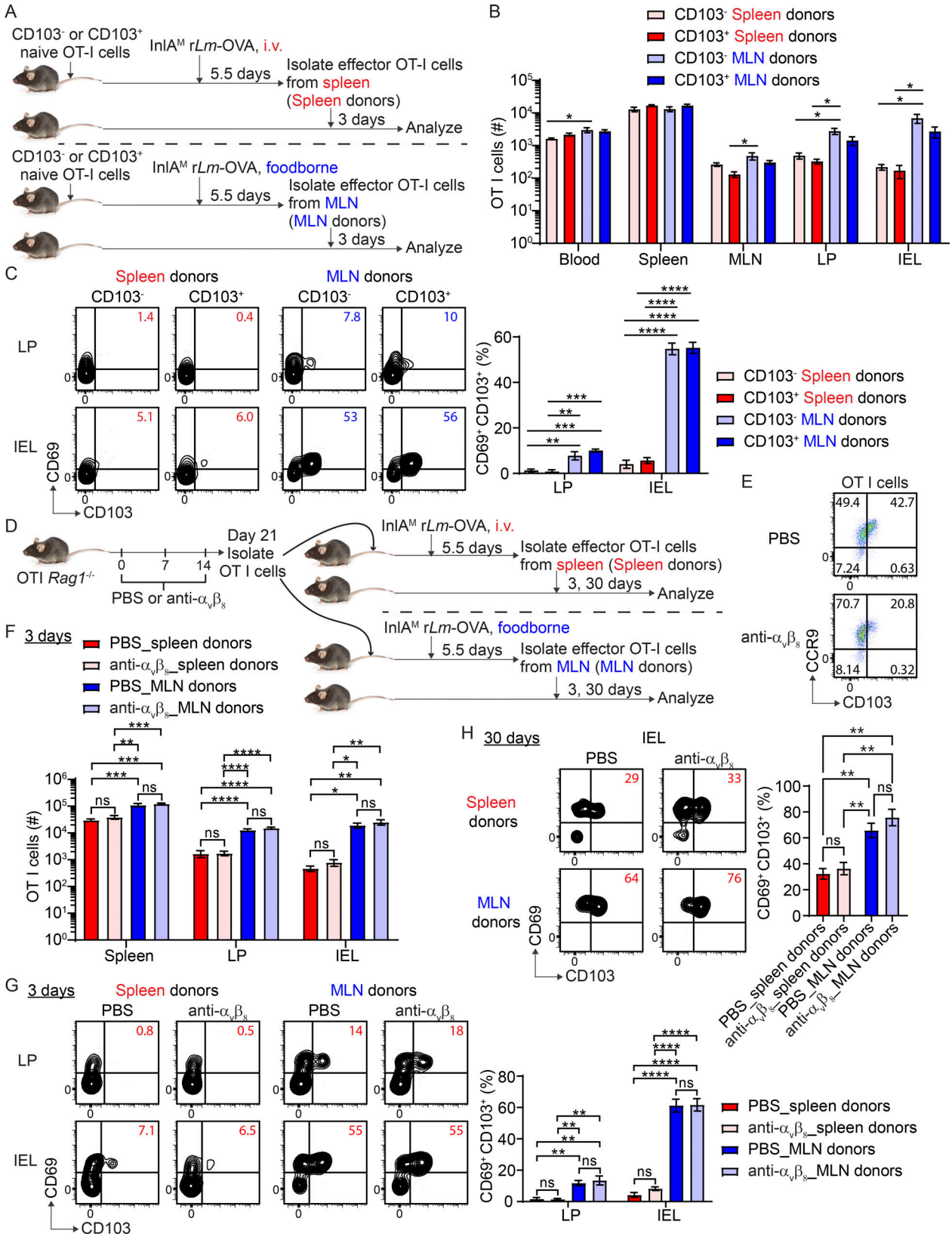

Figure 3. **Preconditioning is not a major determinant of rapid CD103⁺ CD8 T_{RM} cell differentiation in the intestine. (A)** Experimental design for B and C. 2 × 10^4 FACS sorted naive CD103⁺ or CD103⁻ OT-I cells were transferred into congenic naive first recipient mice 1 d prior to i.v. or foodborne infection with InlA^M *Lm*-OVA. At 5.5 dpi, 3 × 10^5 sorted spleen donors or MLN donors were transferred into congenic naive second recipient mice. 3 d after transfer, donor OT-I cells in the second recipient mice were analyzed. **(B)** Numbers of donor OT-I cells in indicated tissues at 3 d after transfer. **(C)** The expression of CD69 and CD103 by donor OT-I cells in the LP and IEL compartment at 3 d after transfer. **(D)** Experimental design for E–H. OT-I *Rag1*$^{-/-}$ mice were intraperitoneally

injected with PBS control or 10 mg/kg anti-$\alpha_v\beta_8$ weekly for 3 wk. 1×10^4 naive OT-I cells were isolated from the spleen of PBS or anti-$\alpha_v\beta_8$ treated OT-I *Rag1*$^{-/-}$ mice and transferred into congenic naive first recipient mice 1 d prior to i.v. or foodborne infection with InlA^M *Lm*-OVA. At 5.5 dpi, spleen donors (3×10^5 for early time point and 5×10^6 for memory time point) or MLN donors (1×10^5 for early time point and 2×10^6 for memory time point) were sorted and transferred into congenic naive second recipient mice. 3 and 30 d after transfer, donor OT-I cells in the second recipient mice were analyzed. **(E)** The expression of CD103 and CCR9 by naive OT-I cells after PBS and anti-$\alpha_v\beta_8$ treatment. **(F)** Numbers of donor OT-I cells (normalized to 5×10^5 transferred cells) in indicated tissues at 3 d after transfer. **(G)** The expression of CD69 and CD103 by donor OT-I cells in the LP and IEL compartment at 3 d after transfer. **(H)** The expression of CD69 and CD103 by donor OT-I cells in the IEL compartment 30 d after transfer. For B and C, n = 3–4 mice/experiment, and similar results were observed in two other experiments. The data in E are representative of three independent experiments. The data in F and G are pooled from two independent experiments, n = 4 mice total. The data in H are pooled from two independent experiments, n = 3–5 mice total. The data are expressed as mean ± SEM. One-way ANOVA with Tukey's multiple comparisons test was performed (B, C, and F–H). *, P ≤ 0.05; **, P ≤ 0.01; ***, P ≤ 0.001; ****, P ≤ 0.0001.

IEL compartment (Ericsson et al., 2004). To determine the impact of CCR9 on CD103$^+$ CD8 T_{RM} cell differentiation in the intestine, naive CD45.1/2$^+$ WT and CD45.2$^+$ *Ccr9*$^{-/-}$ OT-I cells were co-transferred (1:1 ratio) into CD45.1$^+$ recipient mice 1 d prior to foodborne or i.v. infection with InlA^M r*Lm*-OVA. At 8 dpi and memory (>30 d), WT and *Ccr9*$^{-/-}$ T cells were analyzed in recipient mice (Fig. 5 A). Consistent with previous studies that demonstrated a role of CCR9 in directing effector CD8 T cells to the LP and epithelium of the small intestine (Johansson-Lindbom et al., 2003; Stenstad et al., 2007; Wurbel et al., 2007), *Ccr9*$^{-/-}$ OT-I cells were two- and eightfold less efficient than WT OT-I cells in migrating into the LP and IEL compartment after foodborne infection, respectively (Fig. 5 B). Compared with WT OT-I cells, *Ccr9*$^{-/-}$ OT-I cells had a significantly reduced ability to differentiate into CD103$^+$ T_{RM} precursor cells (Fig. 5 C) and CD103$^+$ T_{RM} cells (Fig. 5 D) in the intestine after foodborne infection. Thus, CCR9 promoted intestinal CD103$^+$ CD8 T_{RM} cell differentiation. In line with the observations that spleen-primed OT-I cells did not express appreciable levels of CCR9 (Fig. 1 B and Fig. S2 C), lack of *Ccr9* gene expression did not hinder competitive migration into the LP or IEL compartment or the differentiation of CD103$^+$ CD8 T_{RM} cells after i.v. infection (Fig. 5, B–D).

To further confirm the role of CCR9 in promoting effector CD8 T cell migration to the intestine and the subsequent CD103$^+$ T_{RM} cell differentiation, $\alpha_4\beta_7^-$ CCR9$^-$, $\alpha_4\beta_7^+$ CCR9$^-$, and $\alpha_4\beta_7^+$ CCR9$^+$ effector OT-I cells were sorted from the MLN after foodborne infection and transferred into naïve mice followed by analysis 3 and 30 d (memory) later (Fig. 5 E). $\alpha_4\beta_7^+$ CCR9$^-$ but not $\alpha_4\beta_7^-$ CCR9$^-$ OT-I cells migrated efficiently into the LP (Fig. 5 F), substantiating a critical role for $\alpha_4\beta_7$ in CD8 T cell migration to the LP (Lefrançois et al., 1999). In addition, significantly more $\alpha_4\beta_7^+$ CCR9$^+$ OT-I cells accumulated in the LP and IEL compartment compared with $\alpha_4\beta_7^+$ CCR9$^-$ OT-I cells (Fig. 5 F), corroborating that CCR9 promoted CD8 T cell migration to the LP and especially the IEL compartment. Importantly, $\alpha_4\beta_7^+$ CCR9$^+$ OT-I cells more efficiently differentiated into CD103$^+$ T_{RM} precursor cells at 3 d (Fig. 5 G) and CD103$^+$ T_{RM} cells at 30 d (Fig. 5 H) than $\alpha_4\beta_7^-$ CCR9$^-$ and $\alpha_4\beta_7^+$ CCR9$^-$ OT-I cells, confirming that CCR9 contributed to the development of CD103$^+$ T_{RM} cells in the intestine. However, it should be noted that although not as efficient as $\alpha_4\beta_7^+$ CCR9$^+$ OT-I cells, both $\alpha_4\beta_7^-$ CCR9$^-$ and $\alpha_4\beta_7^+$ CCR9$^-$ OT-I cells were similarly capable of differentiating into intestinal CD103$^+$ T_{RM} precursor cells and CD103$^+$ T_{RM} cells, especially in the IEL compartment (Fig. 5, G and H), suggesting that the differentiation of CD103$^+$ T_{RM} cells in the intestine is regulated by both CCR9-dependent and -independent mechanisms and that $\alpha_4\beta_7$ expression did not impact CD103$^+$ T_{RM} cell differentiation.

We next determined whether CCR9 promoted CD103$^+$ T_{RM} cell differentiation by directly regulating CD103 expression. Naive CD45.1/2$^+$ WT and CD45.2$^+$ *Ccr9*$^{-/-}$ OT-I cells were co-transferred into CD45.1$^+$ recipient mice 1 d prior to foodborne infection with InlA^M r*Lm*-OVA. At 5.5 dpi, cells were isolated from the MLN and in vitro cultured in the presence or absence of TGF-β for 24 h followed by flow analysis of CD103 protein expression (Fig. 5 I). In response to TGF-β, *Ccr9*$^{-/-}$ OT-I cells upregulated CD103 expression as efficiently as WT OT-I cells (Fig. 5 J), suggesting that *Ccr9*$^{-/-}$ T cells were fully competent to upregulate CD103 expression in response to TGF-β in vitro. However, *Ccr9*$^{-/-}$ OT-I cells were impaired in their ability to upregulate CD103 expression and differentiate into CD103$^+$ T_{RM} cells in vivo (Fig. 5, C and D). Thus, these data suggest that CCR9 contributes to intestinal CD103$^+$ T_{RM} cell differentiation likely by localizing effector CD8 T cells to microregions in the intestine where TGF-β is abundant.

Licensing of intestinal CD103$^+$ T_{RM} cell differentiation occurs through RA signaling with minor contribution from CCR9

We next sought to determine the mechanism of intestinal CD103$^+$ T_{RM} cell licensing. At least five of the most upregulated genes in MLN-primed T cells (*Ccr9*, *Hic 1*, *Itgae* and *Lztfl1*, *P2rx7*) can be induced by RA (Burrows et al., 2017; Hashimoto-Hill et al., 2017; Heiss et al., 2008; Iliev et al., 2009; Iwata et al., 2004; Jiang et al., 2016; Fig. 4 D), suggesting that RA may be important for gut CD103$^+$ T_{RM} cell licensing. RA is metabolized from retinol (vitamin A) through a two-step oxidation process (O'Byrne and Blaner, 2013). Retinol is first oxidized to retinal by retinol dehydrogenases and retinal is subsequently oxidized to RA by retinal dehydrogenases (RALDH). MLN but not spleen DC express RALDH2 and are capable of converting retinol to RA and providing RA to instruct CD8 T cells to express $\alpha_4\beta_7$ and CCR9 (Iwata et al., 2004; Svensson et al., 2008). To determine whether RA signals during T cell priming in the MLN licensed CD103$^+$ CD8 T_{RM} cell differentiation, mice were treated with DMSO or a pan-RA receptor (RAR) antagonist AGN194310 to block RA signaling during T cell priming in the MLN after foodborne infection (Fig. 6 A). Alternatively, mice were treated with DMSO or RARα/β agonist AM80 to stimulate RA signaling during T cell priming in the spleen after i.v. infection. Treated MLN-primed and spleen-primed T cells were sorted at 5.5 dpi and transferred into naive congenic recipient mice followed by analysis 3 and 30 d (memory) later. Consistent with the role of RA in inducing $\alpha_4\beta_7$ and CCR9 expression on CD8 T cells, MLN-primed T cells

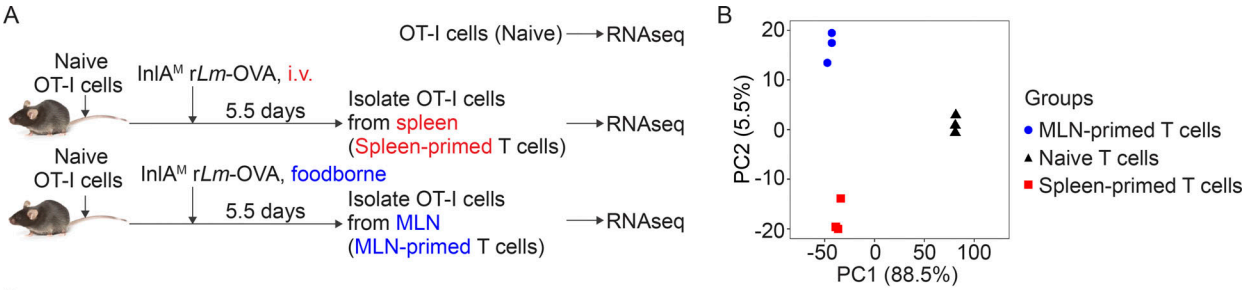

D

Gene	Description	MLN-primed/Spleen-primed fold change
Ccr9	Chemokine (C-C motif) receptor 9	18.82
Hic1	Hypermethylated in cancer 1	3.65
Car2	Carbonic anhydrase 2	3.50
Batf3	Basic leucine zipper transcription factor, ATF-like 3	3.30
Itgae	Integrin alpha E, epithelial-associated	3.24
Lztfl1	Leucine zipper transcription factor-like 1	3.15
Xcl1	Chemokine (C motif) ligand 1	3.11
P2rx7	purinergic receptor P2X, ligand-gated ion channel 7	3.10
Npm1	nucleophosmin 1	2.85
Rangrf	RAN guanine nucleotide release factor	2.83

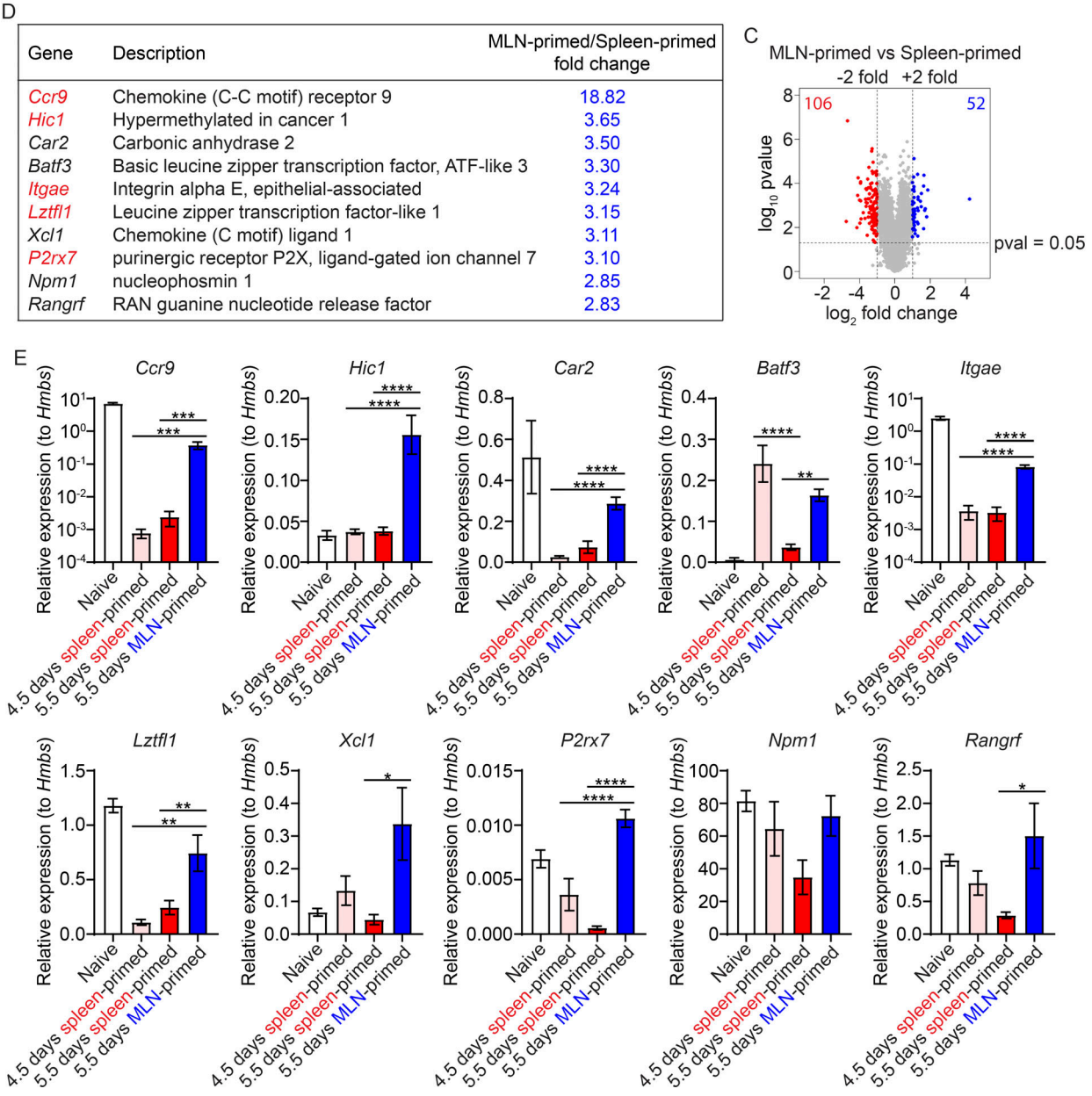

Figure 4. **A CD103⁺ T_{RM} cell gene signature is initiated prior to emigration from the MLN. (A)** Experimental design. 1 × 10^4 naive OT-I cells were transferred into congenic naive recipient mice 1 d prior to i.v. or foodborne infection with InlA^M *Lm*-OVA. At 5.5 dpi, sorted spleen donors or MLN donors were subjected to RNA extraction and RNA sequencing (RNAseq). Naive OT-I cells were used as a control. **(B)** Principal component analysis comparing spleen-primed T cells, MLN-primed T cells, and naive T cells. **(C)** Volcano plot analysis comparing spleen-primed T cells and MLN-primed T cells. **(D)** Top 10 most upregulated genes in MLN-primed T cells compared to spleen-primed T cells. Those in red can be induced by retinoic acid. **(E)** Quantitative PCR confirmation of these top 10 most upregulated genes. Relative expression to the housekeeping gene *Hmbs* was calculated. The data in B–D were generated using biological replicates from three independent experiments. The data in E are pooled from three independent experiments and expressed as mean ± SEM, *n* = 4–10 mice total. Comparisons among 4.5-d spleen-primed, 5.5-d spleen-primed, and 5.5-d MLN-primed groups were performed using one-way ANOVA with Tukey's multiple comparisons test. *, P ≤ 0.05; **, P ≤ 0.01; ***, P ≤ 0.001; ****, P ≤ 0.0001.

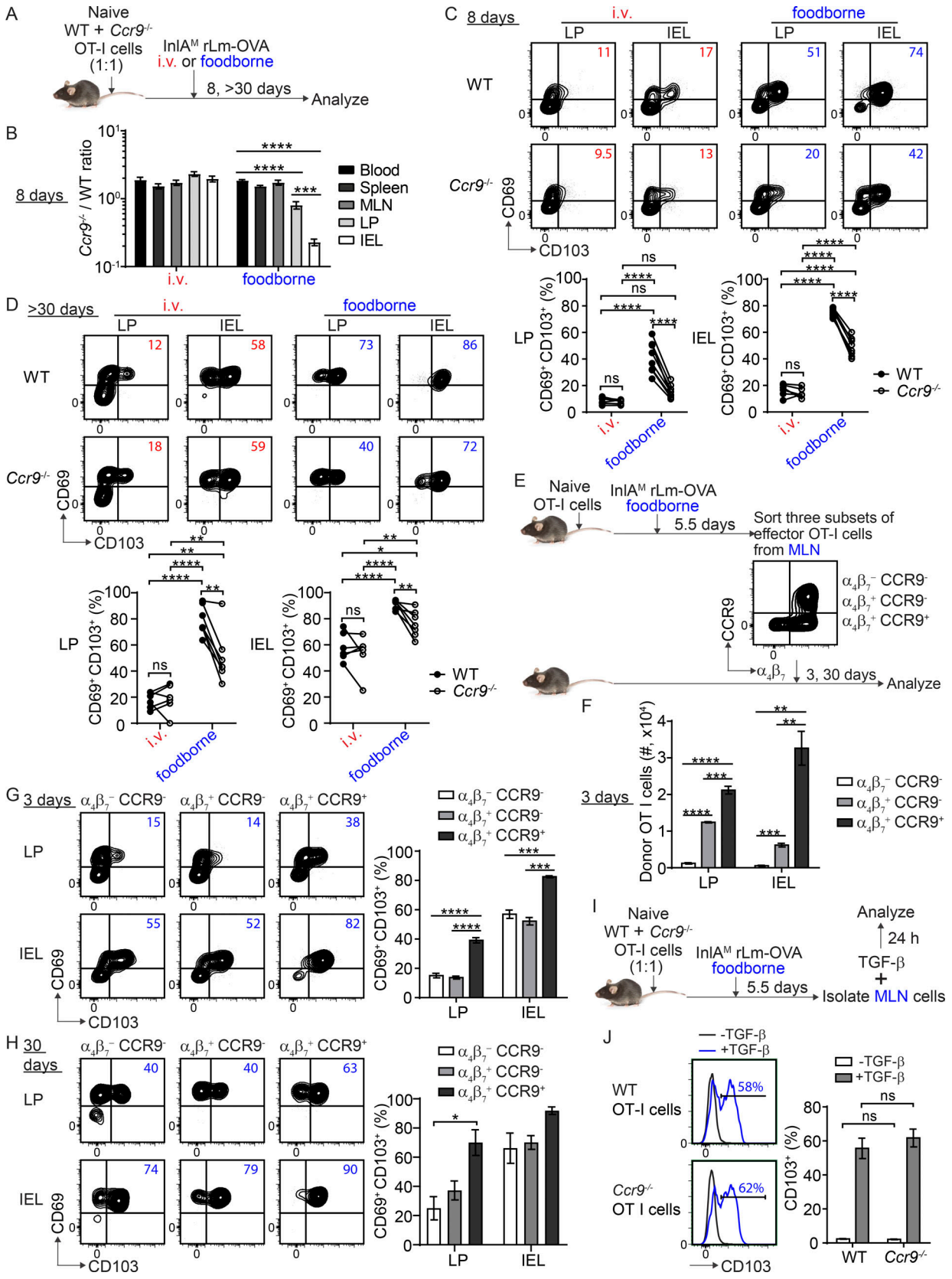

Figure 5. **CCR9 expression contributes to intestinal CD103⁺ T_{RM} cell differentiation. (A)** Experimental design for B–D. 1 × 10^4 CD45.1/2⁺ WT OT-I cells from OT-I *Rag1*$^{-/-}$ mice and 1 × 10^4 CD45.2⁺ *Ccr9*$^{-/-}$ OT-I cells from *Ccr9*$^{-/-}$ OT-I *Rag1*$^{-/-}$ mice were co-transferred into CD45.1⁺ recipient mice 1 d prior to foodborne or i.v. infection with InlA^M *r*Lm-OVA. At 8 and >30 dpi, WT and *Ccr9*$^{-/-}$ T cells were analyzed in recipient mice. **(B)** Numbers of WT and *Ccr9*$^{-/-}$ OT-I cells in indicated tissues at 8 dpi. **(C)** The expression of CD69 and CD103 by WT and *Ccr9*$^{-/-}$ OT-I cells in the LP and IEL compartment at 8 dpi. **(D)** The

expression of CD69 and CD103 by WT and *Ccr9*$^{-/-}$ OT-I cells in the LP and IEL compartment at >30 dpi. **(E)** Experimental design for F–H. 1 × 10^4 naive OT-I cells were transferred into congenic naive first recipient mice 1 d prior to foodborne infection with InlA^M *Lm*-OVA. At 5.5 dpi, $\alpha_4\beta_7^-$ CCR9$^-$, $\alpha_4\beta_7^+$ CCR9$^-$, and $\alpha_4\beta_7^+$ CCR9$^+$ effector OT-I cells were sorted from the MLN and transferred into congenic naive second recipient mice. 3 and 30 d after transfer, donor OT-I cells in the second recipient mice were analyzed. **(F)** Numbers of indicated donor OT-I cells in the LP and IEL compartment at 3 d after transfer. **(G)** The expression of CD69 and CD103 by indicated donor OT-I cells in the LP and IEL compartment at 3 d after transfer. **(H)** The expression of CD69 and CD103 by indicated donor OT-I cells in the LP and IEL compartment 30 d after transfer. **(I)** Experimental design for J. 1 × 10^4 CD45.1/2$^+$ WT OT-I cells and 1 × 10^4 CD45.2$^+$ *Ccr9*$^{-/-}$ OT-I cells were cotransferred into CD45.1$^+$ recipient mice 1 d prior to foodborne infection with InlA^M r*Lm*-OVA. At 5.5 dpi, MLN cells were in vitro cultured in the presence or absence of TGF-β for 24 h followed by flow analysis of CD103 protein expression. **(J)** The expression of CD103 by WT and *Ccr9*$^{-/-}$ T cells. The data in B and C are pooled from two independent experiments, *n* = 6–8 mice total. The data in D are pooled from two independent experiments, *n* = 6–7 mice total. The data in F and G are representative of three independent experiments, *n* = 3 mice/experiment. The data in H are pooled from three independent experiments, *n* = 3 mice total. The data in J are representative of two independent experiments, *n* = 3 mice/experiment. Each dot in C and D depicts one individual mouse. The data in B, F, G, H, and J are expressed as mean ± SEM. One-way ANOVA with Tukey's multiple comparisons test was performed (B, F, G, and H). Paired *t* tests were performed (C and D). Two-way ANOVA with Sidak's multiple comparisons test was performed between WT and *Ccr9*$^{-/-}$ groups (J). Only comparisons between blood and other groups as well as between LP and IEL are shown (B). *, P ≤ 0.05; **, P ≤ 0.01; ***, P ≤ 0.001; ****, P ≤ 0.0001.

treated with AGN194310 had almost completely abolished $\alpha_4\beta_7$ and CCR9 expression, while spleen-primed T cells treated with AM80 had significantly increased $\alpha_4\beta_7$ and CCR9 expression (Fig. 6 B). Consequently, treatment with AGN194310 led to impaired accumulation of MLN-primed T cells in the LP and IEL compartment, while treatment with AM80 resulted in enhanced accumulation of spleen-primed T cells in these compartments (Fig. S5 A). We next determined whether modulating RA signaling during T cell priming had an impact on intestinal CD103$^+$ CD8 T_{RM} cell differentiation. Of note, neither AGN194310 nor AM80 treatment affected KLRG-1 expression (Fig. S5 B). Strikingly, AGN194310 treatment inhibited MLN-primed T cells from differentiating into CD103$^+$ T_{RM} precursor cells at 3 d and CD103$^+$ T_{RM} cells at 30 d in the intestine (Fig. 6, C and D), suggesting RA signaling is necessary for CD103$^+$ T_{RM} cell licensing. Of note, AGN194310 treatment also inhibited spleen-primed T cells from differentiating into CD103$^+$ T_{RM} precursor cells (Fig. S5, C and D). In contrast, AM80 treatment rendered spleen-primed T cells the ability to differentiate into intestinal CD103$^+$ T_{RM} precursor cells at 3 d and CD103$^+$ T_{RM} cells at 30 d to the same level as MLN-primed T cells (Fig. 6, C and D), suggesting RA signaling is sufficient to license CD103$^+$ T_{RM} cell differentiation. Of note, AM80 treatment also enhanced the ability of MLN-primed T cells to rapidly differentiate into intestinal CD103$^+$ T_{RM} precursor cells (Fig. S5, C and D). Thus, these data provide compelling evidence that RA signals during MLN priming license intestinal CD103$^+$ T_{RM} cell differentiation.

We next examined whether RA signaling regulated CD103$^-$ T_{RM} cell differentiation. While blocking RA signaling using AGN194310 significantly inhibited the differentiation of MLN-primed T cells into CD103$^-$ T_{RM} precursor cells in the LP at 3 d (Fig. S5 E), stimulating RA signaling using AM80 significantly inhibited the differentiation of spleen-primed T cells into CD103$^-$ T_{RM} cells in the IEL compartment at 30 d (Fig. S5 F). Overall, the impact of RA signaling on CD103$^-$ T_{RM} cell differentiation appears less substantial and more variable.

Since RA plays a crucial role in inducing CCR9 expression on CD8 T cells, and both CCR9-dependent and -independent mechanisms contributed to CD103$^+$ T_{RM} cell differentiation (Fig. 5, G and H), we sought to determine the relative contribution of CCR9-dependent and -independent mechanisms to RA-licensed intestinal CD103$^+$ T_{RM} cell differentiation. To this end, WT and *Ccr9*$^{-/-}$ naive OT-I cells were transferred into congenic mice 1 d prior to i.v. infection (Fig. 6 E). Mice were treated with DMSO or AM80 during T cell priming. At 5.5 dpi, spleen-primed T cells were sorted and transferred into naive congenic recipient mice followed by analysis at 3 and 30 d (memory) later. As expected, while AM80 treatment drastically increased $\alpha_4\beta_7$ expression in both WT and *Ccr9*$^{-/-}$ T cells, it only induced CCR9 expression in WT but not *Ccr9*$^{-/-}$ T cells (Fig. 6 F). As a result, AM80 treatment led to a significantly enhanced accumulation of WT T cells in both the LP and IEL compartment (Fig. S5 G). However, the accumulation of *Ccr9*$^{-/-}$ T cells in the LP and IEL compartment was only slightly enhanced (Fig. S5 G), consistent with the findings that CCR9 promotes CD8 T cell migration to both compartments. AM80 treatment during T cell priming rendered spleen-primed WT T cells the ability to differentiate into intestinal CD103$^+$ T_{RM} precursor cells at 3 d and CD103$^+$ T_{RM} cells at 30 d (Fig. 6, G and H). Intriguingly, AM80 treatment also enabled *Ccr9*$^{-/-}$ T cells to differentiate into intestinal CD103$^+$ T_{RM} precursor cells at 3 d and CD103$^+$ T_{RM} cells at 30 d (Fig. 6, G and H). The ability of *Ccr9*$^{-/-}$ T cells to differentiate into CD103$^+$ T_{RM} precursor cells and CD103$^+$ T_{RM} cells in the IEL compartment was at ∼75% of the level of WT T cells (Fig. 6, G and H). Thus, RA signaling licensed intestinal CD103$^+$ T_{RM} cell differentiation, primarily driven by factors other than CCR9 induction and CCR9-mediated gut homing.

RA signaling modulates intestinal CD103$^+$ T_{RM} cell formation after infection

As RA signaling is sufficient and necessary for intestinal CD103$^+$ T_{RM} cell differentiation, we next determined whether we could modulate RA signaling to alter CD103$^+$ T_{RM} cell formation in the intestine without secondary transfer to determine whether this pathway has the potential for therapeutic manipulation. 1 × 10^4 naive OT-I cells were transferred into congenic naive recipient mice. 1 d later, mice were i.v. or foodborne infected with InlA^M *Lm*-OVA. For i.v. infection, mice were treated with DMSO or AM80 at 0.5, 2.5, and 4.5 dpi. For foodborne infection, mice were treated with DMSO or AGN194310 at 0.5, 2.5, and 4.5 dpi. Donor OT-I cells were analyzed at >30 dpi (Fig. 7 A). Comparisons between DMSO-treated groups demonstrated that i.v. infection led to significantly less CD103$^+$ T_{RM} cells in the LP and IEL compartment than foodborne infection (Fig. 7 B). Importantly, stimulation of RA signaling with AM80 significantly enhanced CD103$^+$ T_{RM} cell formation after i.v. infection, and

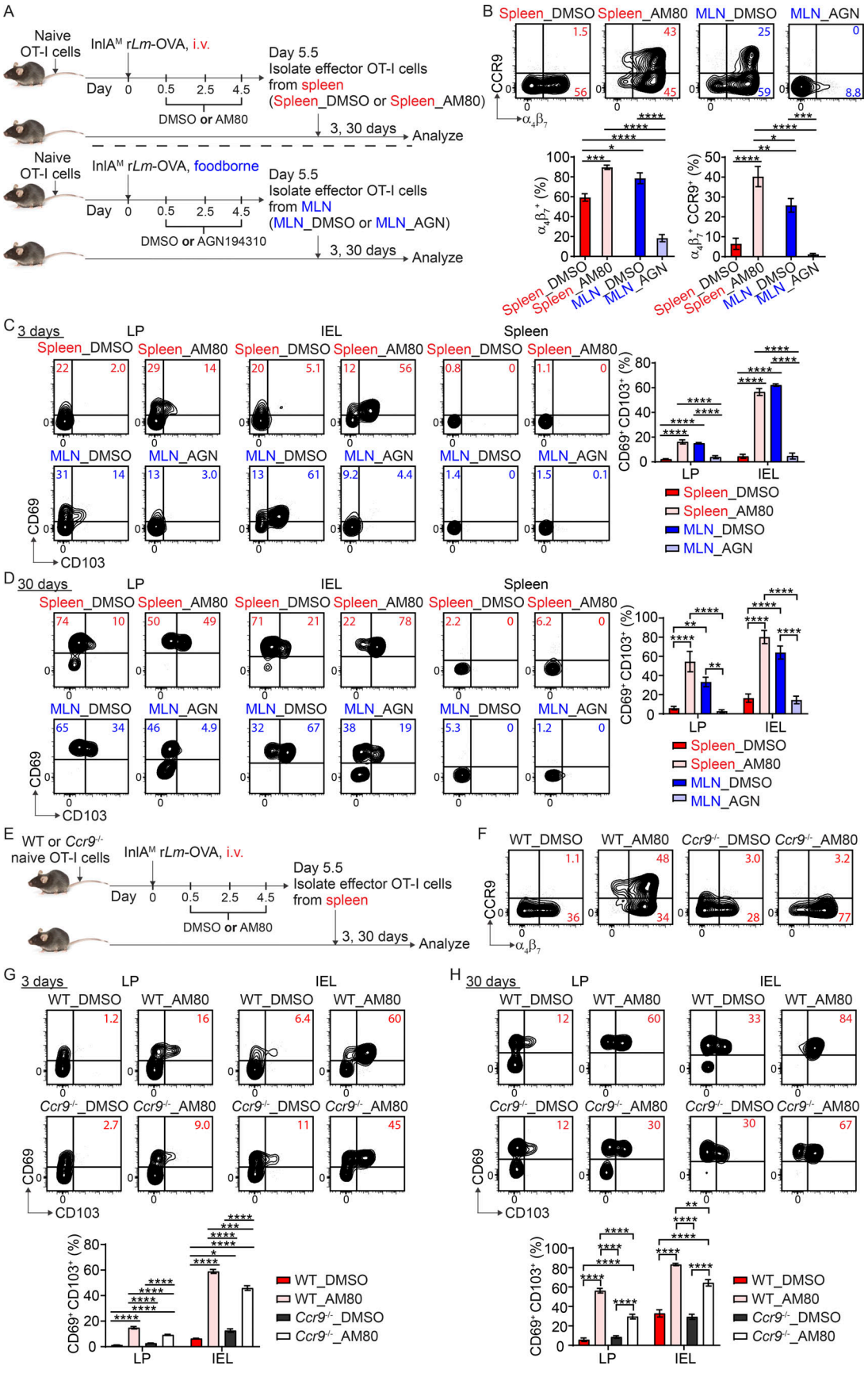

Figure 6. **Licensing of rapid intestinal CD103⁺ T_{RM} cell differentiation occurs through RA signaling that is primarily driven by factors other than CCR9. (A)** Experimental design for B–D. 1 × 10^4 naive OT-I cells were transferred into congenic naive first recipient mice 1 d prior to i.v. or foodborne infection

with InlA^M *Lm*-OVA. For i.v. infection, mice were treated with DMSO control or AM80 at 0.5, 2.5, and 4.5 dpi. For foodborne infection, mice were treated with DMSO control or AGN194310 at 0.5, 2.5, and 4.5 dpi. At 5.5 dpi, effector OT-I cells were sorted from the spleen of i.v.-infected mice treated with DMSO (Spleen_DMSO) or AM80 (Spleen_AM80) or from the MLN of foodborne infected mice treated with DMSO (MLN_DMSO) or AGN194310 (MLN_AGN) and transferred into congenic naive second recipient mice. 3 and 30 d after transfer, donor OT-I cells in the second recipient mice were analyzed. **(B)** The expression of $\alpha_4\beta_7$ and CCR9 by effector OT-I cells prior to adoptive transfer into the second recipient mice. **(C)** The expression of CD69 and CD103 by donor OT-I cells in the LP and IEL compartment at 3 d after transfer. **(D)** The expression of CD69 and CD103 by donor OT-I cells in the LP and IEL compartment 30 d after transfer. **(E)** Experimental design for F–H. 1 × 10^4 WT or *Ccr9*$^{-/-}$ OT-I cells were transferred into congenic naive first recipient mice 1 d prior to i.v. infection with InlA^M *Lm*-OVA. Mice were treated with DMSO control or AM80 at 0.5, 2.5, and 4.5 dpi. At 5.5 dpi, WT and *Ccr9*$^{-/-}$ effector OT-I cells were sorted from the spleen of DMSO treated (WT_DMSO or *Ccr9*$^{-/-}$_DMSO) or AM80 treated (WT_AM80 or *Ccr9*$^{-/-}$_AM80) mice and transferred into congenic naive second recipient mice. 3 and 30 d after transfer, donor OT-I cells in the second recipient mice were analyzed. **(F)** The expression of $\alpha_4\beta_7$ and CCR9 by effector OT-I cells prior to adoptive transfer into second recipient mice. **(G)** The expression of CD69 and CD103 by donor OT-I cells in the LP and IEL compartment at 3 d after transfer. **(H)** The expression of CD69 and CD103 by donor OT-I cells in the LP and IEL compartment 30 d after transfer. The data in B are pooled from three independent experiments, *n* = 5–6 mice total. The data in C are representative of two independent experiments, *n* = 4 mice/experiment. The data in D are pooled from four independent experiments, *n* = 6–8 mice total. The data in F are representative of four independent experiments. The data in G are representative of two independent experiments, *n* = 4 mice/experiment. The data in H are pooled from two independent experiments, *n* = 5 total. The data are expressed as mean ± SEM. One-way ANOVA with Tukey's multiple comparisons test was performed (B–D, G, and H). *, P ≤ 0.05; **, P ≤ 0.01; ***, P ≤ 0.001; ****, P ≤ 0.0001.

AGN194310 treatment that inhibits RA signaling reduced CD103$^+$ T_{RM} cell formation after foodborne infection (Fig. 7 B). These data indicated that CD103$^+$ T_{RM} cell formation could be altered by modifying RA signaling.

Discussion

Developing vaccine strategies to target induction of robust CD8 T_{RM} cell populations is a topic of ongoing clinical interest. As such, understanding the mechanisms that regulate the development of CD8 T_{RM} cells in their unique environments is paramount to facilitate the ability to generate and manipulate these cells for therapeutic benefits. This is especially relevant to current vaccine strategies targeting gastrointestinal infections and tumors that are primarily delivered parenterally. It is generally accepted that priming dictates the migratory pattern of effector CD8 T cells by instruction with tissue-homing receptors (Park and Kupper, 2015; Sheridan and Lefrançois, 2011). Priming in the MLN promotes the migration of effector CD8 T cells to the intestine, providing a crucial layer regulating effector CD8 T cell

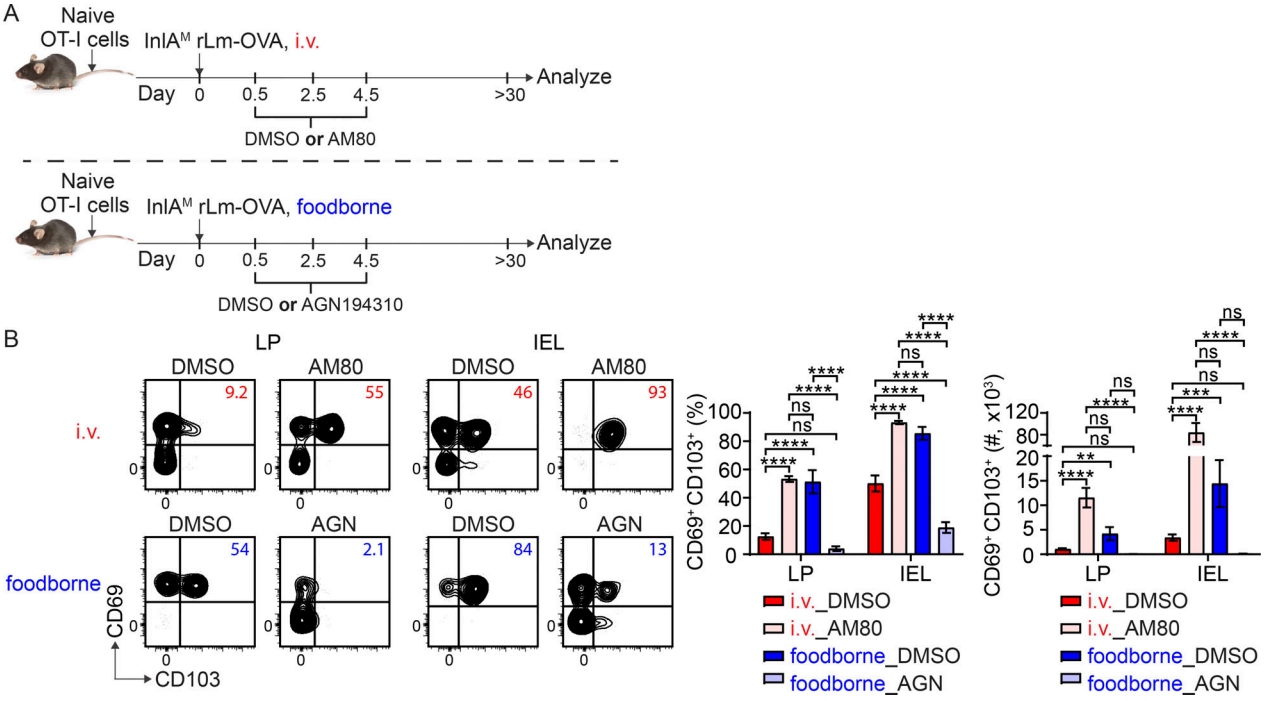

Figure 7. **RA signaling modulates intestinal CD103$^+$ T_{RM} cell formation after infection. (A)** Experimental design. 1 × 10^4 naive OT-I cells were transferred into congenic naive recipient mice. 1 d later, mice were i.v. or foodborne infected with InlA^M *Lm*-OVA. For i.v. infection, mice were treated with DMSO control or AM80 at 0.5, 2.5, and 4.5 dpi. For foodborne infection, mice were treated with DMSO control or AGN194310 at 0.5, 2.5, and 4.5 dpi. Donor OT-I cells were analyzed at >30 dpi. **(B)** The percentage and number of CD69$^+$ CD103$^+$ donor OT-I cells in the LP and IEL compartment at 30 dpi. The data are representative of two independent experiments, *n* = 6–8 mice/experiment. The data are expressed as mean ± SEM. One-way ANOVA with Tukey's multiple comparisons test was performed. **, P ≤ 0.01; ***, P ≤ 0.001; ****, P ≤ 0.0001.

responses in the gut. While spleen-primed CD8 T cells are less efficient at gut homing, CD8 T cells that are primed in the spleen are still detectable in gut tissues. Here, our data established that priming in the MLN also promotes in situ CD103$^+$ CD8 T_{RM} cell differentiation in the intestine, providing an additional regulatory layer for the development of effector and memory CD8 T cell responses in the gut. MLN priming but not spleen priming promoted CD8 T cell differentiation into CD103$^+$ T_{RM} cells in the intestinal LP and epithelium. Consistent with previous studies (Masopust et al., 2006), unique cues from the intestinal environmental induced CD103$^+$ T_{RM} cell differentiation as MLN-primed T cells that migrated to the spleen after adoptive transfer did not become CD103$^+$ T_{RM} cells. Importantly, spleen-primed CD8 T cells that migrated to the intestine were inefficient at becoming CD103$^+$ T_{RM} cells in the intestinal environment. Thus, compelling evidence was provided to demonstrate that priming in the MLN licensed effector CD8 T cells to respond to environmental cues in the intestine to efficiently differentiate into CD103$^+$ T_{RM} cells. We further demonstrated that MLN priming initiated a T_{RM} cell signature before emigration from the MLN and licensed rapid CD103$^+$ T_{RM} cell differentiation through RA signaling. Although CCR9 promoted CD103$^+$ T_{RM} cell differentiation to some extent, RA signaling primarily regulated intestinal CD103$^+$ T_{RM} cell differentiation through other CCR9-independent mechanisms. Therefore, our study established that RA signaling during T cell priming in the MLN promotes CD103$^+$ T_{RM} cell differentiation in the gut.

Our data also demonstrated that in addition to priming, the MLN could impart an environment signal to promote effector CD8 T cell differentiation into CD103$^+$ T_{RM} precursor cells in the intestine. However, this mechanism was not as efficient as priming in the MLN for the induction of intestinal CD103$^+$ CD8 T_{RM} cells. MLN stromal cells can also express high levels of RALDH and convert retinol to RA to support the induction of gut-homing T cells (Hammerschmidt et al., 2008; Molenaar et al., 2009). Therefore, it is possible that RA derived from stromal cells contributes to the intrinsic environment of the MLN that contributes to CD103$^+$ T_{RM} precursor cell licensing.

Previous studies demonstrated that intranasal infection of $InlA^M$ r*Lm* is inefficient at promoting gut CD103$^+$ T_{RM} cell differentiation (Sheridan et al., 2014), corroborating the critical role of MLN priming in regulating intestinal CD103$^+$ T_{RM} cell differentiation. However, whether this is unique to the gut and gut-draining lymph nodes requires further studies. The skin environment alone appears sufficient for CD103$^+$ T_{RM} cell differentiation regardless of whether CD8 T cells are primed in vivo or activated in vitro (Mackay et al., 2013; Mackay et al., 2012). A recent study demonstrated that α_V-expressing migratory DC activate and present TGF-β to naive CD8 T cells during homeostasis to precondition them to become skin CD103$^+$ T_{RM} cells upon priming (Mani et al., 2019). Spleen-primed effector CD8 T cells generated with i.v. r*Lm*-OVA infection efficiently differentiated into CD103$^+$ T_{RM} cells after being pulled into the skin epidermis by topical treatment with an inflammation-inducing agent. However, our study provides strong evidence that preconditioning does not contribute to CD103$^+$ T_{RM} cell differentiation in the intestine. These distinctions highlight the complexity and unique biology that individual tissues contribute to T_{RM} cell development.

TGF-β is essential for the differentiation of CD103$^+$ CD8 T_{RM} cells in the intestine as CD8 T cells deficient in TGF-β receptor II are not able to differentiate into intestinal CD103$^+$ T_{RM} cells (Casey et al., 2012; Sheridan et al., 2014; Zhang and Bevan, 2013). Our data showed that RA plays an important role in licensing effector CD8 T cell responsiveness to factors in the intestinal environment for differentiation into CD103$^+$ T_{RM} cells. However, how RA signaling received during MLN priming regulates CD103$^+$ CD8 T_{RM} cell differentiation in the intestine in response to TGF-β needs further exploration. Our data demonstrate that MLN priming provided RA signaling to license CD103$^+$ T_{RM} cell differentiation to a limited extent through a CCR9-dependent mechanism. In addition to directing the migration of effector CD8 T cells to the intestine, CCR9 likely further direct effector T cells that have already infiltrated the intestine to microanatomical areas where TGF-β is abundant, although the detailed mechanism requires further studies. However, a CCR9-independent mechanism appears to play the major role in licensing CD103$^+$ T_{RM} cell development as CCR9$^-$ MLN-primed effector CD8 T cells as well as AM80-treated spleen-primed *Ccr9*$^{-/-}$ effector CD8 T cells were capable of differentiating into CD103$^+$ T_{RM} cells. RA has been shown to directly induce CD103 expression on DC (Iliev et al., 2009), although this is unlikely to be the case for CD8 T cells as effector CD8 T cells that received RA signaling either through MLN-priming or RARα/β agonism did not upregulate CD103 expression after entering the spleen. RA has been shown to induce *Hic1* expression on T cells, and T cell–intrinsic expression of *Hic1* promotes CD103$^+$ resident LP lymphocytes and IEL during homeostasis (Burrows et al., 2017). A recent study also showed that *Hic1* is upregulated in T_{RM} cells in the IEL compartment after infection and regulates T_{RM} cell formation (Crowl et al., 2022). Since our data showed that *Hic1* expression was upregulated in MLN-primed but not spleen-primed CD8 T cells prior to migration to the intestine, it is possible that RA signaling received during priming in the MLN promotes the differentiation of CD103$^+$ T_{RM} cells in the intestine through *Hic1*. RA is produced both in the intestinal epithelium and the MLN (Iliev et al., 2009; Iwata et al., 2004); therefore, effector CD8 T cells can receive RA signaling either during priming or after migration into the intestine to upregulate *Hic1*. Our data clearly showed that RA signaling received during priming is critical for intestinal CD103$^+$ T_{RM} cell differentiation. However, it is unclear whether RA signaling received in the intestine also contributes to T_{RM} cell formation or homeostasis. Furthermore, AM80 treatment rendered the ability of spleen-primed CD8 T cells to differentiate into CD103$^+$ T_{RM} cells, indicating that spleen-primed CD8 T cells can respond to RA. However, whether their inability to differentiate into CD103$^+$ T_{RM} cells is due to the lack of RA signaling during priming or their inability to see RA after migrating into the intestine requires further investigation. RA has also been shown to induce *P2rx7* expression (Hashimoto-Hill et al., 2017; Heiss et al., 2008), and *P2rx7* promotes CD103$^+$ CD8 T_{RM} cell generation and maintenance by upregulating CD103 and enabling the ability of CD8 T cells to respond to TGF-β (Borges da Silva et al., 2020). Our data showed that *P2rx7* was one of the top 10 most upregulated genes in MLN-primed T cells. Therefore, RA signaling

received during priming in the MLN may also contribute to intestinal CD103$^+$ T_{RM} cell differentiation through *P2rx7*. A recent study showed that changes in *Hic1* expression lead to changes in *P2rx7* expression (Crowl et al., 2022), suggesting that RA regulation of *P2rx7* expression can be both direct and indirect. In all, it is possible that RA signaling orchestrates multiple pathways collectively contributing to the differentiation of intestinal CD103$^+$ T_{RM} cells.

Overall, our study provides crucial insight into the mechanism regulating intestinal CD103$^+$ CD8 T_{RM} cell development that may shed light on rational vaccine design targeting infections and cancers of gastrointestinal tract. It emphasizes the importance of utilizing oral immunization route to target MLN priming for generating robust CD103$^+$ CD8 T_{RM} cell population in the intestine and provides a new regime to modulate RA signaling to tailor the development of these cells for potential therapeutic applications.

Materials and methods

Mice

C57BL/6 mice for experiments without OT-I cell transfer were purchased from The Jackson Laboratory. C57BL/6 mice expressing the congenic markers CD45.1 or CD45.2 for experiments with OT-I cell transfer were purchased from the Charles River-National Cancer Institute. OT-I *Rag1*$^{-/-}$ mice expressing CD45.1, CD45.2, or both and *Ccr9*$^{-/-}$ OT-I *Rag1*$^{-/-}$ mice expressing CD45.2 were bred and maintained at Stony Brook University under specific-pathogen-free conditions. For experiments using *Ccr9*$^{-/-}$ OT-I *Rag1*$^{-/-}$ mice, WT OT-I *Rag1*$^{-/-}$ mice were used as controls. 8–12-wk-old, age-matched female mice were used in experiments. All animal procedures were carried out in accordance with National Institutes of Health (NIH) guidelines and approved by the Stony Brook University Institutional Animal Care and Use Committee.

Bacteria

L. monocytogenes strain 10403s carrying a mutation in the internalin A protein and expressing a truncated form of OVA (InlA^M r*Lm*-OVA) have been described previously (Plumlee et al., 2013). Prior to infection, mice were deprived of food and water for 6 h. Foodborne infection was performed by providing ~1 cm^3 piece of bread inoculated with 2 × 10^9 cfu of InlA^M r*Lm*-OVA in PBS to individually housed mice (Chu et al., 2022). I.v. infection was performed by tail vein injection of 2 × 10^3 cfu of InlA^M r*Lm*-OVA in PBS.

Adoptive transfers

1 × 10^4 CD45.1$^+$ OT-I cells isolated from the spleen of OT-I *Rag1*$^{-/-}$ mice were i.v. transferred into naive CD45.2$^+$ recipient mice 1 d prior to i.v. or foodborne infection with InlA^M r*Lm*-OVA. 5.5 d after infection, unless otherwise specified, effector OT-I cells were isolated from the spleen of i.v.-infected mice and the MLN of foodborne-infected mice based on the congenic marker CD45.1. Briefly, tissues were mashed through 70-µm cell strainers (Falcon) to obtain single-cell suspension. Cells were stained with anti-CD45.1-biotin (A20; BioLegend) followed by incubation with anti-biotin microbeads (Miltenyi Biotec) and enrichment on a MACS Separator (Miltenyi Biotec). After enrichment, cells were stained with the following fluorophore-conjugated antibodies from BioLegend or Invitrogen: anti-CD4 (GK1.5), anti-MHC II (M5/114.15.2), anti-CD8α (53–6.7), anti-CD45.1 (A20), anti-CD45.2 (104), and live/dead dye (Invitrogen) for fluorescence-activated cell sorting. Single, live, CD4$^-$ MHC II$^-$ CD8α$^+$ CD45.2$^-$ CD45.1$^+$ effector OT-I cells were sorted using a FACSARIA III cell sorter (BD). The purity after sorting was consistently >95%. 2-5 × 10^5 (for early time point) or 2-5 × 10^6 (for memory time point) effector OT-I cells were transferred intravenously into indicated CD45.2$^+$ recipient mice unless otherwise indicated. Alternatively, CD45.2$^+$ OT-I cells and CD45.1$^+$ recipient mice were used. For WT and *Ccr9*$^{-/-}$ OT-I cotransfer experiments, 1 × 10^4 CD45.1/2$^+$ WT OT-I cells from OT-I *Rag1*$^{-/-}$ mice and 1 × 10^4 CD45.2$^+$ *Ccr9*$^{-/-}$ OT-I cells from *Ccr9*$^{-/-}$ OT-I *Rag1*$^{-/-}$ mice were cotransferred into CD45.1$^+$ recipient mice.

Lymphocyte isolation

To isolate lymphocytes from the spleen and MLN, tissues were mashed through 70-µm cell strainers. Small intestine LP lymphocytes and IEL were isolated as previously described (Qiu and Sheridan, 2018; Sheridan and Lefrançois, 2012). Briefly, small intestines were cut into 1-inch long pieces after removal of Peyer's patches and luminal content. Intestinal tissues were treated twice with 1 mM dithioerythritol (Sigma-Aldrich) solution in a shaker at 220 rpm and 37°C for 20 min. Supernatants were collected, combined, and subjected to 44%/67% Percoll (GE Healthcare) gradient for the isolation of IEL. The remaining intestine tissues were treated twice with 1.3 mM ethylenediaminetetraacetic acid (Invitrogen) solution in a shaker at 220 rpm and 37°C for 30 min to remove intestinal epithelial cells, followed by digestion with 100 U/ml of collagenase (Invitrogen) in a shaker at 300 rpm and 37°C for 45 min. Supernatants were collected after collagenase digestion and the undigested tissues were mashed through 70-µm cell strainers into the collected supernatant, which was then subjected to 44%/67% Percoll gradient for the isolation of LP lymphocytes.

Flow cytometry and antibodies

The following fluorophore-conjugated antibodies from BioLegend, Invitrogen, or BD Biosciences were used: anti-CD45 (30-F11), anti-TCRβ (H57-597), anti-CD8α (53–6.7), anti-CD11a (M17/4), anti-CD45.1 (A20), anti-CD45.2 (104), anti-CD103 (2E7), anti-CD69 (H1.2F3), anti-α4β7 (DATK32), anti-CCR9 (CW-1.2), and anti-KLRG-1 (2F1/KRLG1). Live/dead dye was purchased from Invitrogen. H-2 K^b OVA_{257} monomer was obtained from the NIH Tetramer Core Facility and tetramerized in-house using fluorophore-conjugated streptavidin (Invitrogen). Cells were stained with antibodies at 4°C in the dark for 20 min. If tetramer was used, staining was performed at room temperature in the dark for 1 h. After staining, cells were fixed with 2% paraformaldehyde (Electron Microscopy Sciences) for 20 min prior to acquisition on a LSRFortessa (BD) or an Aurora (Cytek). Data were analyzed with FlowJo software (Tree Star).

FTY720 treatment

FTY720 (Cayman Chemical) was dissolved in PBS with 25% DMSO. Mice were injected intraperitoneally with vehicle control or 1 mg/kg FTY720 daily for 3 wk.

Anti-$\alpha_v\beta_8$ treatment

Anti-$\alpha_v\beta_8$ (ADWA-11) was kindly provided by Dr. Dean Sheppard (University of California, San Francisco). Mice were injected intraperitoneally with PBS control or 10 mg/kg anti-$\alpha_v\beta_8$ weekly for 3 wk.

RNA sequencing and data processing

RNA was extracted using QIAGEN RNeasy Plus Micro Kit. Libraries were prepared using Illumina TruSeq Stranded mRNA library kit at the Center for Genome Innovation at UCONN Storrs, CT, USA. RNA sequencing and data analysis were performed by Macrogen. Fold changes were calculated based on $\log_2$(FPKM+1). Principle component analysis and volcano plot analysis were performed using R.

Quantitative PCR

RNA was isolated using RNeasy Plus Micro Kit (QIAGEN) and cDNA was generated using iScript Advanced cDNA Synthesis Kit (Bio-Rad). Real-time RT-PCR was performed on a Bio-Rad CFX96 using PrimePCR Assays purchased from Bio-Rad (qMmuCID0009067 for *Ccr9*, qMmuCED0040393 for *Hic1*, qMmuCID0019169 for *Car2*, qMmuCID0020840 for *Batf3*, qMmuCID0039603 for *Itgae*, qMmuCID0026896 for *Lztfl1*, qMmuCID0006409 for *Xcl1*, qMmuCID0040113 for *P2rx7*, qMmuCED0041023 for *Npm1*, qMmuCED0061466 for *Rangrf*, and qMmuCID0022816 for *Hmbs*).

In vitro culture

4×10^6 cells isolated from the MLN after foodborne infection or from the spleen after i.v. infection were cultured in the absence or presence of 5 ng/ml TGF-β1 (Peprotech), unless otherwise specified, in a 48-well plate with 250 µl culture medium per well for 24 h. RPMI medium 1640 (Gibco) supplemented with 10% FBS (Gibco), 1% GlutaMAX (Gibco), 10 mM Hepes (Gibco), 1 mM sodium pyruvate (Gibco), 100 units/ml penicillin (Gibco), 100 µg/ml streptomycin (Gibco), 20 µg/ml gentamicin (Gibco), and 50 µM 2-mercaptoethanal (Sigma-Aldrich) was used as culture medium.

Chemical modulation of RA signaling

Mice were injected intraperitoneally with DMSO, 5 mg/kg RARα/β agonist AM80 (Sigma-Aldrich), or 1 mg/kg pan-RAR antagonist AGN194310 every other day starting at day 0.5 until euthanization. The dosage was determined based on previous studies and our own titration experiments (Allie et al., 2013; Matsushita et al., 2011).

Bacterial burdens

Spleen and MLN were mashed through 70-µm cell strainers (Thermo Fisher Scientific) using sterile 1% saponin (Calbiochem). Gut tissues were disassociated using C Tubes and gentleMACS Dissociator (Miltenyi Biotec) in nine volumes of sterile PBS. After disassociation, 1 volume of sterile 10% saponin was added. Tissue homogenates were incubated at 4°C for 1 h before plating on BHI agar plates supplemented with 200 µg/ml streptomycin. Bacterial colonies were enumerated 24–48 h after incubation at 37°C.

Statistical analysis

All statistical analyses were performed in Prism (GraphPad Software) using two-tailed Student's *t* test for comparisons of two groups and one-way ANOVA for comparisons of more than two groups. *, $P \le 0.05$; **, $P \le 0.01$; ***, $P \le 0.001$; ****, $P \le 0.0001$.

Online supplemental material

Fig. S1 shows the expression of CD69 and CD103 by effector OT-I cells prior to entry into the intestine, the impact of priming on CD103$^-$ T_{RM} precursor cell differentiation, and the impact of intrinsic environment of the MLN on CD103$^+$ T_{RM} precursor cell differentiation. Fig. S2 shows that rapid intestinal CD103$^+$ CD8 T_{RM} precursor cell differentiation is independent of activation stage, intestinal homing, and KLRG-1 expression. Fig. S3 demonstrates the impact of infection on intestinal CD103$^+$ T_{RM} cell differentiation and the residency of intestinal memory CD8 T cells derived from spleen-primed T cells. Fig. S4 demonstrates the sorting strategy for CD103$^-$ and CD103$^+$ naive OT-I cells, the expression of CD69 and CD103 by transferred CD103$^-$ and CD103$^+$ naive OT-I cells after activation, and the ability to upregulate CD103 expression in response to TGF-β by spleen and MLN donors. Fig. S5 shows the effect of RA signaling modulation on effector T cell migration to the intestine, KLRG-1 expression, and T_{RM} precursor cell differentiation.

Data availability

RNA sequencing data in Fig. 4 has been deposited in Gene Expression Omnibus with the accession number GSE223983. All other data are available from the corresponding author.

Acknowledgments

We thank Drs. Adrianus van der Velden (Stony Brook University) and Pawan Kumar (Stony Brook University) for constructive discussion on the manuscript. We acknowledge the support of the NIH Tetramer Core Facility for providing MHC I monomers and Dr. Dean Sheppard (University of California, San Francisco, San Francisco, CA, USA) for providing the anti-$\alpha_v\beta_8$ antibody. Graphical abstract was created with Biorender.com.

This study was supported by NIH awards K12GM102778 (Z. Qiu), P01AI056172 (L. Puddington), R01AI076457 (B.S. Sheridan), R01AI172919 (B.S. Sheridan), R21AI137929 (B.S. Sheridan), and funds provided by Stony Brook University (B.S. Sheridan).

Author contributions: B.S. Sheridan and Z. Qiu directed and designed the study. Z. Qiu, C. Khairallah, T.H. Chu, J.N. Imperato, X. Lei, and G. Romanov performed the experiments. L. Puddington and A. Atakilit provided resources. Z. Qiu analyzed the data. Z. Qiu and B.S. Sheridan wrote the manuscript.

Disclosures: The authors declare no competing interests exist.

Submitted: 29 April 2021
Revised: 2 December 2022
Accepted: 1 February 2023

References

Allie, S.R., W. Zhang, C.Y. Tsai, R.J. Noelle, and E.J. Usherwood. 2013. Critical role for all-trans retinoic acid for optimal effector and effector memory CD8 T cell differentiation. *J. Immunol.* 190:2178–2187. https://doi.org/10.4049/jimmunol.1201945

Ariotti, S., M.A. Hogenbirk, F.E. Dijkgraaf, L.L. Visser, M.E. Hoekstra, J.Y. Song, H. Jacobs, J.B. Haanen, and T.N. Schumacher. 2014. T cell memory. Skin-resident memory CD8+ T cells trigger a state of tissue-wide pathogen alert. *Science.* 346:101–105. https://doi.org/10.1126/science.1254803

Bankovich, A.J., L.R. Shiow, and J.G. Cyster. 2010. CD69 suppresses sphingosine 1-phosophate receptor-1 (S1P1) function through interaction with membrane helix 4. *J. Biol. Chem.* 285:22328–22337. https://doi.org/10.1074/jbc.M110.123299

Bergsbaken, T., and M.J. Bevan. 2015. Proinflammatory microenvironments within the intestine regulate the differentiation of tissue-resident CD8+ T cells responding to infection. *Nat. Immunol.* 16:406–414. https://doi.org/10.1038/ni.3108

Bergsbaken, T., M.J. Bevan, and P.J. Fink. 2017. Local inflammatory cues regulate differentiation and persistence of CD8+ tissue-resident memory T cells. *Cell Rep.* 19:114–124. https://doi.org/10.1016/j.celrep.2017.03.031

Best, J.A., D.A. Blair, J. Knell, E. Yang, V. Mayya, A. Doedens, M.L. Dustin, A.W. Goldrath, and Immunological Genome Project Consortium. 2013. Transcriptional insights into the CD8(+) T cell response to infection and memory T cell formation. *Nat. Immunol.* 14:404–412. https://doi.org/10.1038/ni.2536

Borges da Silva, H., C. Peng, H. Wang, K.M. Wanhainen, C. Ma, S. Lopez, A. Khoruts, N. Zhang, and S.C. Jameson. 2020. Sensing of ATP via the purinergic receptor P2RX7 promotes CD8+ trm cell generation by enhancing their sensitivity to the cytokine TGF-β. *Immunity.* 53:158–171.e6. https://doi.org/10.1016/j.immuni.2020.06.010

Burrows, K., F. Antignano, M. Bramhall, A. Chenery, S. Scheer, V. Korinek, T.M. Underhill, and C. Zaph. 2017. The transcriptional repressor HIC1 regulates intestinal immune homeostasis. *Mucosal Immunol.* 10:1518–1528. https://doi.org/10.1038/mi.2017.17

Casey, K.A., K.A. Fraser, J.M. Schenkel, A. Moran, M.C. Abt, L.K. Beura, P.J. Lucas, D. Artis, E.J. Wherry, K. Hogquist, et al. 2012. Antigen-independent differentiation and maintenance of effector-like resident memory T cells in tissues. *J. Immunol.* 188:4866–4875. https://doi.org/10.4049/jimmunol.1200402

Cheuk, S., H. Schlums, I. Gallais Sérézal, E. Martini, S.C. Chiang, N. Marquardt, A. Gibbs, E. Detlofsson, A. Introini, M. Forkel, et al. 2017. CD49a expression defines tissue-resident CD8+ T cells poised for cytotoxic function in human skin. *Immunity.* 46:287–300. https://doi.org/10.1016/j.immuni.2017.01.009

Chu, T.H., Z. Qiu, and B.S. Sheridan. 2022. The use of foodborne infection to evaluate bacterial pathogenesis and host response. *Methods Cell Biol.* 168:299–314. https://doi.org/10.1016/bs.mcb.2021.12.020

Crowl, J.T., M. Heeg, A. Ferry, J.J. Milner, K.D. Omilusik, C. Toma, Z. He, J.T. Chang, and A.W. Goldrath. 2022. Tissue-resident memory CD8+ T cells possess unique transcriptional, epigenetic and functional adaptations to different tissue environments. *Nat. Immunol.* 23:1121–1131. https://doi.org/10.1038/s41590-022-01229-8

Dodagatta-Marri, E., H.Y. Ma, B. Liang, J. Li, D.S. Meyer, S.Y. Chen, K.H. Sun, X. Ren, B. Zivak, M.D. Rosenblum, et al. 2021. Integrin αvβ8 on T cells suppresses anti-tumor immunity in multiple models and is a promising target for tumor immunotherapy. *Cell Rep.* 36:109309. https://doi.org/10.1016/j.celrep.2021.109309

Ericsson, A., M. Svensson, A. Arya, and W.W. Agace. 2004. CCL25/CCR9 promotes the induction and function of CD103 on intestinal intraepithelial lymphocytes. *Eur. J. Immunol.* 34:2720–2729. https://doi.org/10.1002/eji.200425125

Ganesan, A.P., J. Clarke, O. Wood, E.M. Garrido-Martin, S.J. Chee, T. Mellows, D. Samaniego-Castruita, D. Singh, G. Seumois, A. Alzetani, et al. 2017. Tissue-resident memory features are linked to the magnitude of cytotoxic T cell responses in human lung cancer. *Nat. Immunol.* 18:940–950. https://doi.org/10.1038/ni.3775

Gebhardt, T., L.M. Wakim, L. Eidsmo, P.C. Reading, W.R. Heath, and F.R. Carbone. 2009. Memory T cells in nonlymphoid tissue that provide enhanced local immunity during infection with herpes simplex virus. *Nat. Immunol.* 10:524–530. https://doi.org/10.1038/ni.1718

Hammerschmidt, S.I., M. Ahrendt, U. Bode, B. Wahl, E. Kremmer, R. Förster, and O. Pabst. 2008. Stromal mesenteric lymph node cells are essential for the generation of gut-homing T cells in vivo. *J. Exp. Med.* 205:2483–2490. https://doi.org/10.1084/jem.20080039

Hashimoto-Hill, S., L. Friesen, M. Kim, and C.H. Kim. 2017. Contraction of intestinal effector T cells by retinoic acid-induced purinergic receptor P2X7. *Mucosal Immunol.* 10:912–923. https://doi.org/10.1038/mi.2016.109

Heiss, K., N. Jänner, B. Mähnss, V. Schumacher, F. Koch-Nolte, F. Haag, and H.W. Mittrücker. 2008. High sensitivity of intestinal CD8+ T cells to nucleotides indicates P2X7 as a regulator for intestinal T cell responses. *J. Immunol.* 181:3861–3869. https://doi.org/10.4049/jimmunol.181.6.3861

Hirai, T., Y. Yang, Y. Zenke, H. Li, V.K. Chaudhri, J.S. De La Cruz Diaz, P.Y. Zhou, B.A. Nguyen, L. Bartholin, C.J. Workman, et al. 2021. Competition for active TGFβ cytokine allows for selective retention of antigen-specific tissue- resident memory T cells in the epidermal niche. *Immunity.* 54:84–98.e5. https://doi.org/10.1016/j.immuni.2020.10.022

Hirai, T., Y. Zenke, Y. Yang, L. Bartholin, L.K. Beura, D. Masopust, and D.H. Kaplan. 2019. Keratinocyte-mediated activation of the cytokine TGF-β maintains skin recirculating memory CD8+ T cells. *Immunity.* 50:1249–1261.e5. https://doi.org/10.1016/j.immuni.2019.03.002

Iliev, I.D., I. Spadoni, E. Mileti, G. Matteoli, A. Sonzogni, G.M. Sampietro, D. Foschi, F. Caprioli, G. Viale, and M. Rescigno. 2009. Human intestinal epithelial cells promote the differentiation of tolerogenic dendritic cells. *Gut.* 58:1481–1489. https://doi.org/10.1136/gut.2008.175166

Imperato, J.N., D. Xu, P.A. Romagnoli, Z. Qiu, P. Perez, C. Khairallah, Q.M. Pham, A. Andrusaite, A. Bravo-Blas, S.W.F. Milling, et al. 2020. Mucosal CD8 T cell responses are shaped by batf3-DC after foodborne *Listeria monocytogenes* infection. *Front. Immunol.* 11:575967. https://doi.org/10.3389/fimmu.2020.575967

Iwata, M., A. Hirakiyama, Y. Eshima, H. Kagechika, C. Kato, and S.Y. Song. 2004. Retinoic acid imprints gut-homing specificity on T cells. *Immunity.* 21:527–538. https://doi.org/10.1016/j.immuni.2004.08.011

Jiang, H., K. Promchan, B.R. Lin, S. Lockett, D. Chen, H. Marshall, Y. Badralmaa, and V. Natarajan. 2016. LZTFL1 upregulated by all-trans retinoic acid during CD4+ T cell activation enhances IL-5 production. *J. Immunol.* 196:1081–1090. https://doi.org/10.4049/jimmunol.1500719

Jiang, X., R.A. Clark, L. Liu, A.J. Wagers, R.C. Fuhlbrigge, and T.S. Kupper. 2012. Skin infection generates non-migratory memory CD8+ T(RM) cells providing global skin immunity. *Nature.* 483:227–231. https://doi.org/10.1038/nature10851

Johansson-Lindbom, B., M. Svensson, M.A. Wurbel, B. Malissen, G. Márquez, and W. Agace. 2003. Selective generation of gut tropic T cells in gut-associated lymphoid tissue (GALT): Requirement for GALT dendritic cells and adjuvant. *J. Exp. Med.* 198:963–969. https://doi.org/10.1084/jem.20031244

Khan, T.N., J.L. Mooster, A.M. Kilgore, J.F. Osborn, and J.C. Nolz. 2016. Local antigen in nonlymphoid tissue promotes resident memory CD8+ T cell formation during viral infection. *J. Exp. Med.* 213:951–966. https://doi.org/10.1084/jem.20151855

Khanna, K.M., J.T. McNamara, and L. Lefrançois. 2007. In situ imaging of the endogenous CD8 T cell response to infection. *Science.* 318:116–120. https://doi.org/10.1126/science.1146291

Kohlmeier, J.E., S.C. Miller, and D.L. Woodland. 2007. Cutting edge: Antigen is not required for the activation and maintenance of virus-specific memory CD8+ T cells in the lung airways. *J. Immunol.* 178:4721–4725. https://doi.org/10.4049/jimmunol.178.8.4721

Kumar, B.V., W. Ma, M. Miron, T. Granot, R.S. Guyer, D.J. Carpenter, T. Senda, X. Sun, S.H. Ho, H. Lerner, et al. 2017. Human tissue-resident memory T cells are defined by core transcriptional and functional signatures in lymphoid and mucosal sites. *Cell Rep.* 20:2921–2934. https://doi.org/10.1016/j.celrep.2017.08.078

Lee, Y.T., J.E. Suarez-Ramirez, T. Wu, J.M. Redman, K. Bouchard, G.A. Hadley, and L.S. Cauley. 2011. Environmental and antigen receptor-derived signals support sustained surveillance of the lungs by pathogen-specific cytotoxic T lymphocytes. *J. Virol.* 85:4085–4094. https://doi.org/10.1128/JVI.02493-10

Lefrançois, L., C.M. Parker, S. Olson, W. Muller, N. Wagner, M.P. Schön, and L. Puddington. 1999. The role of beta7 integrins in CD8 T cell trafficking during an antiviral immune response. *J. Exp. Med.* 189:1631–1638. https://doi.org/10.1084/jem.189.10.1631

Mackay, L.K., A. Braun, B.L. Macleod, N. Collins, C. Tebartz, S. Bedoui, F.R. Carbone, and T. Gebhardt. 2015. Cutting edge: CD69 interference with sphingosine-1-phosphate receptor function regulates peripheral T cell retention. *J. Immunol.* 194:2059–2063. https://doi.org/10.4049/jimmunol.1402256

Mackay, L.K., M. Minnich, N.A. Kragten, Y. Liao, B. Nota, C. Seillet, A. Zaid, K. Man, S. Preston, D. Freestone, et al. 2016. Hobit and Blimp1 instruct a universal transcriptional program of tissue residency in lymphocytes. *Science.* 352:459–463. https://doi.org/10.1126/science.aad2035

Mackay, L.K., A. Rahimpour, J.Z. Ma, N. Collins, A.T. Stock, M.L. Hafon, J. Vega-Ramos, P. Lauzurica, S.N. Mueller, T. Stefanovic, et al. 2013. The developmental pathway for CD103(+)CD8+ tissue-resident memory T cells of skin. *Nat. Immunol.* 14:1294–1301. https://doi.org/10.1038/ni.2744

Mackay, L.K., A.T. Stock, J.Z. Ma, C.M. Jones, S.J. Kent, S.N. Mueller, W.R. Heath, F.R. Carbone, and T. Gebhardt. 2012. Long-lived epithelial immunity by tissue-resident memory T (TRM) cells in the absence of persisting local antigen presentation. *Proc. Natl. Acad. Sci. USA.* 109: 7037–7042. https://doi.org/10.1073/pnas.1202288109

Malik, B.T., K.T. Byrne, J.L. Vella, P. Zhang, T.B. Shabaneh, S.M. Steinberg, A.K. Molodtsov, J.S. Bowers, C.V. Angeles, C.M. Paulos, et al. 2017. Resident memory T cells in the skin mediate durable immunity to melanoma. *Sci. Immunol.* 2:eaam6346. https://doi.org/10.1126/sciimmunol.aam6346

Mani, V., S.K. Bromley, T. Äijö, R. Mora-Buch, E. Carrizosa, R.D. Warner, M. Hamze, D.R. Sen, A.Y. Chasse, A. Lorant, et al. 2019. Migratory DCs activate TGF-β to precondition naïve CD8+ T cells for tissue-resident memory fate. *Science.* 366:366. https://doi.org/10.1126/science.aav5728

Masopust, D., D. Choo, V. Vezys, E.J. Wherry, J. Duraiswamy, R. Akondy, J. Wang, K.A. Casey, D.L. Barber, K.S. Kawamura, et al. 2010. Dynamic T cell migration program provides resident memory within intestinal epithelium. *J. Exp. Med.* 207:553–564. https://doi.org/10.1084/jem.20090858

Masopust, D., V. Vezys, E.J. Wherry, D.L. Barber, and R. Ahmed. 2006. Cutting edge: Gut microenvironment promotes differentiation of a unique memory CD8 T cell population. *J. Immunol.* 176:2079–2083. https://doi.org/10.4049/jimmunol.176.4.2079

Matsushita, H., M. Hijioka, A. Hisatsune, Y. Isohama, K. Shudo, and H. Katsuki. 2011. A retinoic acid receptor agonist Am80 rescues neurons, attenuates inflammatory reactions, and improves behavioral recovery after intracerebral hemorrhage in mice. *J. Cereb. Blood Flow Metab.* 31: 222–234. https://doi.org/10.1038/jcbfm.2010.80

Mohammed, J., L.K. Beura, A. Bobr, B. Astry, B. Chicoine, S.W. Kashem, N.E. Welty, B.Z. Igyártó, S. Wijeyesinghe, E.A. Thompson, et al. 2016. Stromal cells control the epithelial residence of DCs and memory T cells by regulated activation of TGF-β. *Nat. Immunol.* 17:414–421. https://doi.org/10.1038/ni.3396

Molenaar, R., M. Greuter, A.P. van der Marel, R. Roozendaal, S.F. Martin, F. Edele, J. Huehn, R. Förster, T. O'Toole, W. Jansen, et al. 2009. Lymph node stromal cells support dendritic cell-induced gut-homing of T cells. *J. Immunol.* 183:6395–6402. https://doi.org/10.4049/jimmunol.0900311

Mueller, S.N., and L.K. Mackay. 2016. Tissue-resident memory T cells: Local specialists in immune defence. *Nat. Rev. Immunol.* 16:79–89. https://doi.org/10.1038/nri.2015.3

Muschaweckh, A., V.R. Buchholz, A. Fellenzer, C. Hessel, P.A. König, S. Tao, R. Tao, M. Heikenwälder, D.H. Busch, T. Korn, et al. 2016. Antigen-dependent competition shapes the local repertoire of tissue-resident memory CD8+ T cells. *J. Exp. Med.* 213:3075–3086. https://doi.org/10.1084/jem.20160888

Nizard, M., H. Roussel, M.O. Diniz, S. Karaki, T. Tran, T. Voron, E. Dransart, F. Sandoval, M. Riquet, B. Rance, et al. 2017. Induction of resident memory T cells enhances the efficacy of cancer vaccine. *Nat. Commun.* 8:15221. https://doi.org/10.1038/ncomms15221

O'Byrne, S.M., and W.S. Blaner. 2013. Retinol and retinyl esters: Biochemistry and physiology. *J. Lipid Res.* 54:1731–1743. https://doi.org/10.1194/jlr.R037648

Pan, Y., T. Tian, C.O. Park, S.Y. Lofftus, S. Mei, X. Liu, C. Luo, J.T. O'Malley, A. Gehad, J.E. Teague, et al. 2017. Survival of tissue-resident memory T cells requires exogenous lipid uptake and metabolism. *Nature.* 543: 252–256. https://doi.org/10.1038/nature21379

Park, C.O., and T.S. Kupper. 2015. The emerging role of resident memory T cells in protective immunity and inflammatory disease. *Nat. Med.* 21: 688–697. https://doi.org/10.1038/nm.3883

Plumlee, C.R., B.S. Sheridan, B.B. Cicek, and L. Lefrançois. 2013. Environmental cues dictate the fate of individual CD8+ T cells responding to infection. *Immunity.* 39:347–356. https://doi.org/10.1016/j.immuni.2013.07.014

Qiu, Z., T.H. Chu, and B.S. Sheridan. 2021. TGF-β: Many paths to CD103+ CD8 T cell residency. *Cells.* 10:989. https://doi.org/10.3390/cells10050989

Qiu, Z., C. Khairallah, and B.S. Sheridan. 2018. *Listeria monocytogenes*: A model pathogen continues to refine our knowledge of the CD8 T cell response. *Pathogens.* 7:55. https://doi.org/10.3390/pathogens7020055

Qiu, Z., and B.S. Sheridan. 2018. Isolating lymphocytes from the mouse small intestinal immune system. *J. Vis. Exp.* 57281. https://doi.org/10.3791/57281

Sallusto, F., D. Lenig, R. Förster, M. Lipp, and A. Lanzavecchia. 1999. Two subsets of memory T lymphocytes with distinct homing potentials and effector functions. *Nature.* 401:708–712. https://doi.org/10.1038/44385

Schenkel, J.M., K.A. Fraser, L.K. Beura, K.E. Pauken, V. Vezys, and D. Masopust. 2014. T cell memory. Resident memory CD8 T cells trigger protective innate and adaptive immune responses. *Science.* 346:98–101. https://doi.org/10.1126/science.1254536

Schenkel, J.M., K.A. Fraser, V. Vezys, and D. Masopust. 2013. Sensing and alarm function of resident memory CD8+ T cells. *Nat. Immunol.* 14: 509–513. https://doi.org/10.1038/ni.2568

Sheridan, B.S., and L. Lefrançois. 2011. Regional and mucosal memory T cells. *Nat. Immunol.* 12:485–491. https://doi.org/10.1038/ni.2029

Sheridan, B.S. and L. Lefrançois. 2012. Isolation of mouse lymphocytes from small intestine tissues. *Curr. Protoc. Immunol.* 3:3.19.1–3.19.11. https://doi.org/10.1002/0471142735.im0319s99

Sheridan, B.S., Q.M. Pham, Y.T. Lee, L.S. Cauley, L. Puddington, and L. Lefrançois. 2014. Oral infection drives a distinct population of intestinal resident memory CD8(+) T cells with enhanced protective function. *Immunity.* 40:747–757. https://doi.org/10.1016/j.immuni.2014.03.007

Shin, H., and A. Iwasaki. 2012. A vaccine strategy that protects against genital herpes by establishing local memory T cells. *Nature.* 491:463–467. https://doi.org/10.1038/nature11522

Shiow, L.R., D.B. Rosen, N. Brdicková, Y. Xu, J. An, L.L. Lanier, J.G. Cyster, and M. Matloubian. 2006. CD69 acts downstream of interferon-alpha/beta to inhibit S1P1 and lymphocyte egress from lymphoid organs. *Nature.* 440:540–544. https://doi.org/10.1038/nature04606

Skon, C.N., J.Y. Lee, K.G. Anderson, D. Masopust, K.A. Hogquist, and S.C. Jameson. 2013. Transcriptional downregulation of S1pr1 is required for the establishment of resident memory CD8+ T cells. *Nat. Immunol.* 14: 1285–1293. https://doi.org/10.1038/ni.2745

Slütter, B., N. Van Braeckel-Budimir, G. Abboud, S.M. Varga, S. Salek-Ardakani, and J.T. Harty. 2017. Dynamics of influenza-induced lung-resident memory T cells underlie waning heterosubtypic immunity. *Sci. Immunol.* 2:eaag2031. https://doi.org/10.1126/sciimmunol.aag2031

Stenstad, H., M. Svensson, H. Cucak, K. Kotarsky, and W.W. Agace. 2007. Differential homing mechanisms regulate regionalized effector CD8alphabeta+ T cell accumulation within the small intestine. *Proc. Natl. Acad. Sci. USA.* 104:10122–10127. https://doi.org/10.1073/pnas.0700269104

Svensson, M., B. Johansson-Lindbom, F. Zapata, E. Jaensson, L.M. Austenaa, R. Blomhoff, and W.W. Agace. 2008. Retinoic acid receptor signaling levels and antigen dose regulate gut homing receptor expression on CD8+ T cells. *Mucosal Immunol.* 1:38–48. https://doi.org/10.1038/mi.2007.4

Takamura, S., H. Yagi, Y. Hakata, C. Motozono, S.R. McMaster, T. Masumoto, M. Fujisawa, T. Chikaishi, J. Komeda, J. Itoh, et al. 2016. Specific niches for lung-resident memory CD8+ T cells at the site of tissue regeneration enable CD69-independent maintenance. *J. Exp. Med.* 213:3057–3073. https://doi.org/10.1084/jem.20160938

Wakim, L.M., A. Woodward-Davis, and M.J. Bevan. 2010. Memory T cells persisting within the brain after local infection show functional adaptations to their tissue of residence. *Proc. Natl. Acad. Sci. USA.* 107: 17872–17879. https://doi.org/10.1073/pnas.1010201107

Wakim, L.M., A. Woodward-Davis, R. Liu, Y. Hu, J. Villadangos, G. Smyth, and M.J. Bevan. 2012. The molecular signature of tissue resident memory CD8 T cells isolated from the brain. *J. Immunol.* 189:3462–3471. https://doi.org/10.4049/jimmunol.1201305

Wollert, T., B. Pasche, M. Rochon, S. Deppenmeier, J. van den Heuvel, A.D. Gruber, D.W. Heinz, A. Lengeling, and W.D. Schubert. 2007. Extending the host range of *Listeria monocytogenes* by rational protein design. *Cell.* 129:891–902. https://doi.org/10.1016/j.cell.2007.03.049

Wu, T., Y. Hu, Y.T. Lee, K.R. Bouchard, A. Benechet, K. Khanna, and L.S. Cauley. 2014. Lung-resident memory CD8 T cells (TRM) are indispensable for optimal cross-protection against pulmonary virus infection. *J. Leukoc. Biol.* 95:215–224. https://doi.org/10.1189/jlb.0313180

Wurbel, M.A., M. Malissen, D. Guy-Grand, B. Malissen, and J.J. Campbell. 2007. Impaired accumulation of antigen-specific CD8 lymphocytes in chemokine CCL25-deficient intestinal epithelium and lamina propria. *J. Immunol.* 178: 7598–7606. https://doi.org/10.4049/jimmunol.178.12.7598

Zhang, N., and M.J. Bevan. 2012. TGF-β signaling to T cells inhibits autoimmunity during lymphopenia-driven proliferation. *Nat. Immunol.* 13: 667–673. https://doi.org/10.1038/ni.2319

Zhang, N., and M.J. Bevan. 2013. Transforming growth factor-β signaling controls the formation and maintenance of gut-resident memory T cells by regulating migration and retention. *Immunity.* 39:687–696. https://doi.org/10.1016/j.immuni.2013.08.019

Supplemental material

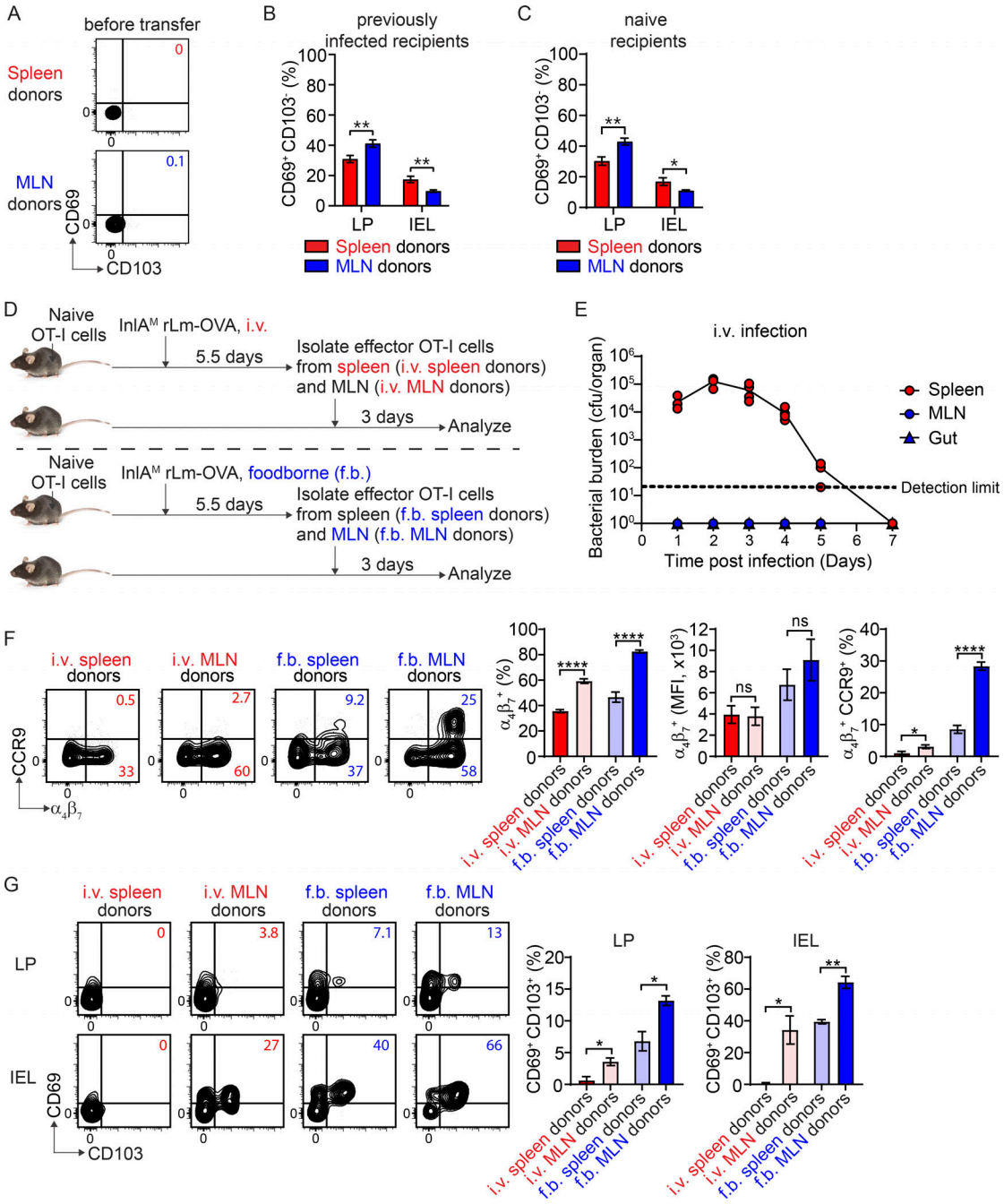

Figure S1. **The expression of CD69 and CD103 by effector OT-I cells prior to entry into the intestine, the impact of priming on CD103⁻ T_{RM} precursor cell differentiation, and the impact of intrinsic environment of the MLN on CD103⁺ T_{RM} precursor cell differentiation. (A)** The expression of CD69 and CD103 by effector OT-I cells prior to adoptive transfer into second recipient mice. **(B)** The percentage of $CD69^+$ $CD103^-$ population in indicated donor OT-I cells in the LP and IEL compartment at 3 d after transfer into second recipient mice that were foodborne $InlA^M$ *Lm*-OVA infected 5.5 d previously. **(C)** The percentage of $CD69^+$ $CD103^-$ population in indicated donor OT-I cells in the LP and IEL compartment at 3 d after transfer into naive second recipient mice. **(D)** Experimental design for F and G. 1×10^4 naive OT-I cells were transferred into congenic naive first recipient mice 1 d prior to i.v. or foodborne infection with $InlA^M$ *Lm*-OVA. At 5.5 dpi, effector OT-I cells were sorted from the spleen and MLN of i.v. infected mice (i.v. spleen donors and i.v. MLN donors) or from the spleen and MLN of foodborne infected mice (f.b. spleen donors and f.b. MLN donors) and transferred into congenic naive second recipient mice. 3 d after transfer, donor OT-I cells in the second recipient mice were analyzed. **(E)** Bacterial burdens in the spleen, MLN, and small intestine (gut) at indicated days after i.v. infection with $InlA^M$ *Lm*-OVA. **(F)** The expression of $\alpha_4\beta_7$ and CCR9 by i.v. spleen donors, i.v. MLN donors, f.b. spleen donors, and f.b. MLN donors prior to adoptive transfer into second recipient mice. **(G)** The expression of CD69 and CD103 by donor OT-I cells in the LP and IEL compartment at 3 d after transfer into second recipient mice. The data in A are representative of three independent experiments. The data in B are pooled from three independent experiments, n = 12–14 mice total. The data in C are pooled from three independent experiments, n = 12 mice total. The data in E are representative of three independent experiments, n = 4–5 mice/experiment. The data in F are pooled from five independent experiments, n = 5 experiments and for each experiment 2–18 mice were pooled for spleen donors and 18–34 mice were pooled for MLN donors. The data in G are representative of two independent experiments, n = 3 mice/experiment. The data are expressed as mean ± SEM and unpaired t tests were performed (B, C, F, and G). *, $P \le 0.05$; **, $P \le 0.01$; ****, $P \le 0.0001$.

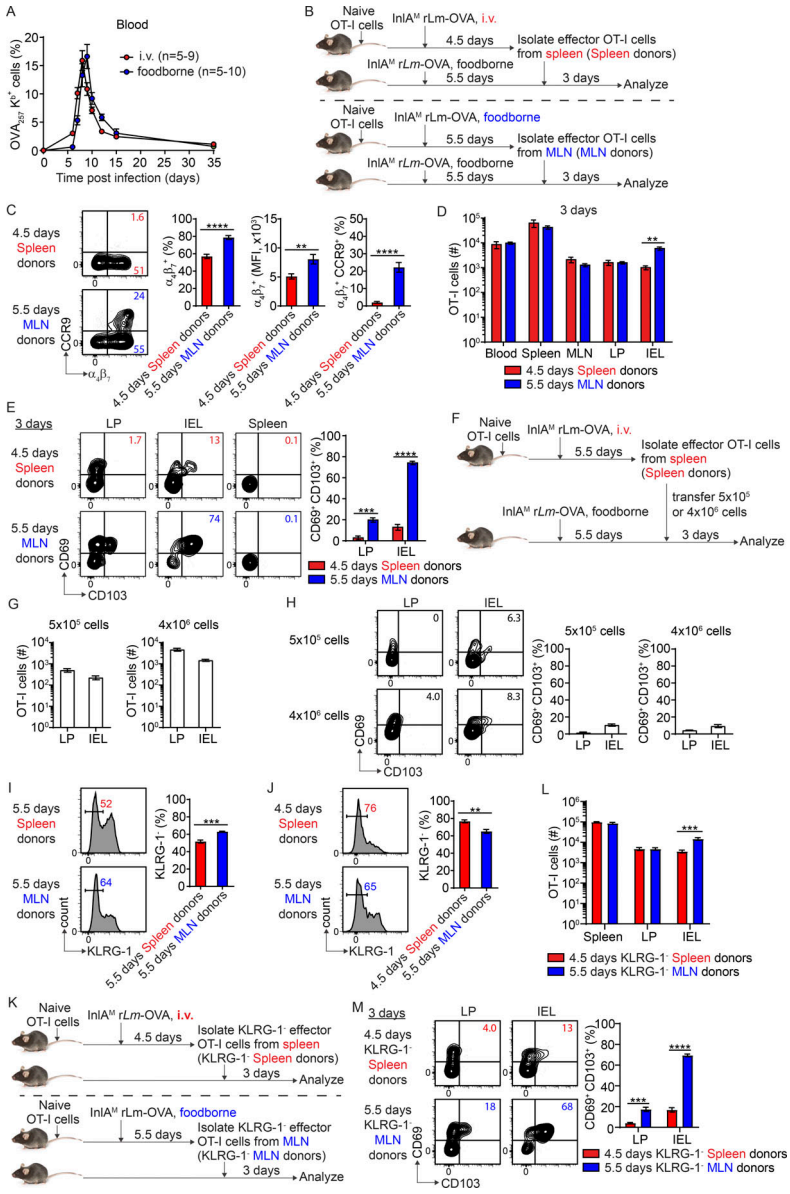

Figure S2. **Rapid intestinal CD103⁺ CD8 T_{RM} precursor cell differentiation is independent of activation stage, intestinal homing, and KLRG-1 expression. (A)** The longitudinal OVA-specific CD8 T cell responses in the blood measured by OVA_{257} K^b tetramer after i.v. and foodborne infection. **(B)** Experimental design for C–E. 1×10^4 naive OT-I cells were transferred into congenic naive first recipient mice. 1 d later, mice were i.v. or foodborne infected with InlA^M *Lm*-OVA. Spleen donors and MLN donors were isolated from the spleen at 4.5 d after i.v. infection and from the MLN at 5.5 d after foodborne infection, respectively. 5×10^5 sorted donor OT-I cells were transferred into congenic second recipient mice that were foodborne InlA^M *Lm*-OVA infected 5.5 d previously. 3 d after transfer, donor OT-I cells in second recipient mice were analyzed. **(C)** The expression of $\alpha_4\beta_7$ and CCR9 by effector OT-I cells prior to adoptive transfer into second recipient mice. **(D)** Numbers of donor OT-I cells in indicated tissues at 3 d after transfer. **(E)** The expression of CD69 and CD103 by donor OT-I cells in the LP and IEL compartment at 3 d after transfer. **(F)** Experimental design for G and H. 1×10^4 naive OT-I cells were transferred into congenic naive first recipient mice 1 d prior to i.v. infection with InlA^M *Lm*-OVA. At 5.5 dpi, 5×10^5 or 4×10^6 sorted Spleen donors were transferred into congenic second recipient mice that were foodborne InlA^M *Lm*-OVA infected 5.5 d previously. 3 d after transfer, donor OT-I cells in second recipient mice were analyzed. **(G)** The accumulation of donor OT-I cells in the LP and IEL compartment at 3 d after transfer. **(H)** The expression of CD69 and CD103 by donor OT-I cells in the LP and IEL compartment at 3 d after transfer. **(I and J)** The percentage of KLRG-1⁻ population in indicated effector OT-I cells prior to adoptive transfer into second recipient mice. **(K)** Experimental design for L and M. 1×10^4 naive OT-I cells were transferred into congenic naive first recipient mice 1 d prior to i.v. or foodborne infection with InlA^M *Lm*-OVA. KLRG-1⁻ Spleen donors and MLN donors were isolated from the spleen at 4.5 d after i.v. infection and from the MLN at 5.5 d after foodborne infection respectively. 5×10^5 sorted donor OT-I cells were transferred into congenic naive second recipient mice. 3 d after transfer, donor OT-I cells in second recipient mice were analyzed. **(L)** Numbers of donor OT-I cells in indicated tissues at 3 d after transfer. **(M)** The expression of CD69 and CD103 by donor OT-I cells in the LP and IEL compartment at 3 d after transfer. The data in A are from one experiment, n = 7–10 mice per infection route and time. The data in C are pooled from three independent experiments, n = 6 mice total. The data in D and E are representative of two independent experiments, n = 4 mice/experiment. The data in G and H are from one experiment, n = 4 mice/experiment. The data in I are pooled from five independent experiments, n = 5 experiments, and for each experiment 2–18 mice were pooled for spleen donors and 18–34 mice were pooled for MLN donors. The data in J are pooled from three independent experiments, n = 6 mice total. The data in L and M are pooled from two independent experiments, n = 6 mice total. The data are expressed as mean ± SEM. Unpaired t tests were performed (C, D, E, and I–L). **, P ≤ 0.01; ***, P ≤ 0.001; ****, P ≤ 0.0001.

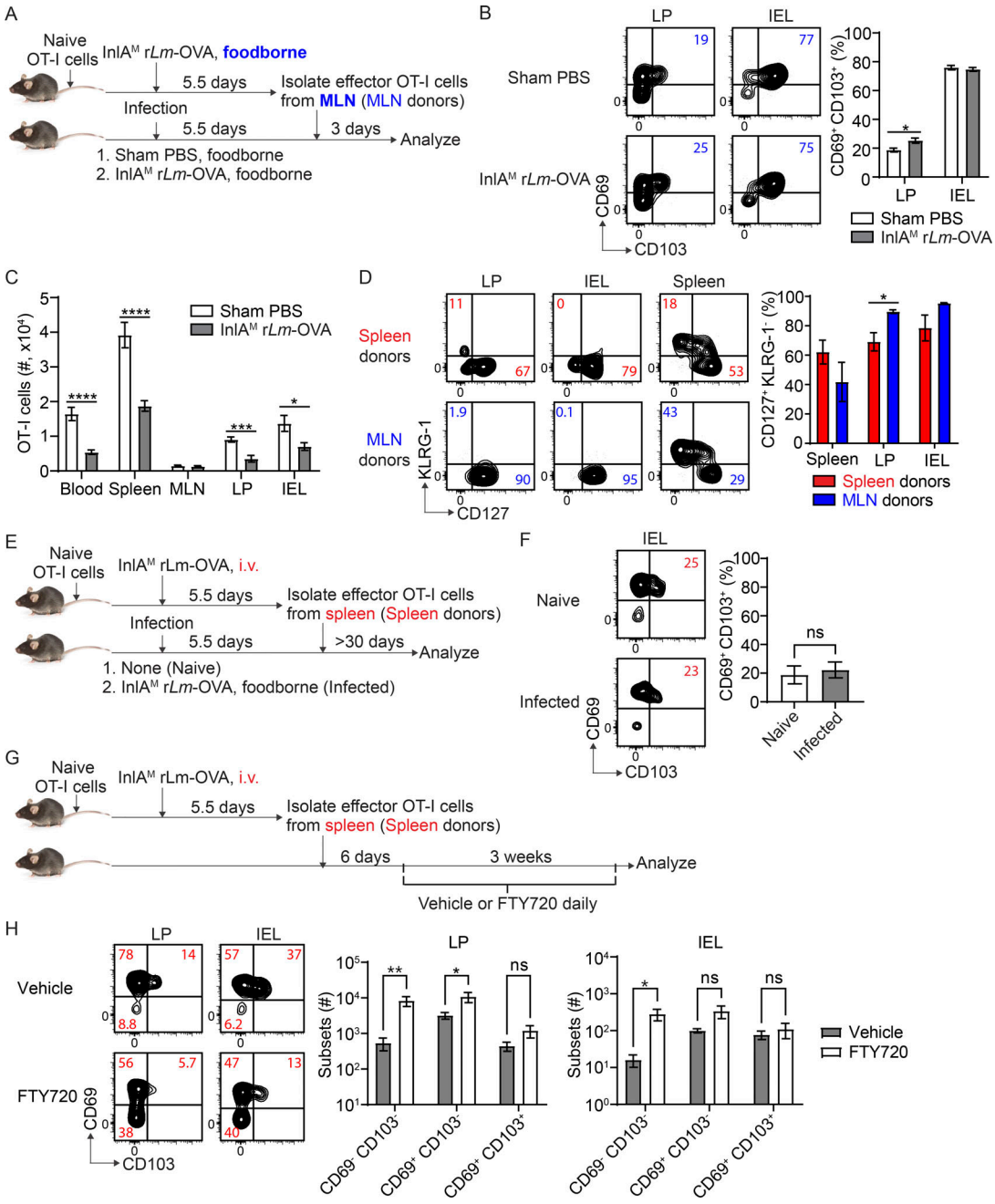

Figure S3. **The impact of infection on intestinal CD103⁺ T_{RM} cell differentiation and the residency of intestinal memory CD8 T cells derived from spleen-primed T cells. (A)** Experimental design for B and C. 1 × 10^4 naive OT-I cells were transferred into congenic naive first recipient mice. 1 d later, mice were foodborne infected with InlA^M *Lm*-OVA. At 5.5 dpi, effector OT-I cells were isolated from the MLN and transferred into congenic second recipient mice that were foodborne infected with InlA^M *Lm*-OVA or treated with sham PBS 5.5 d previously. 3 d after transfer, donor OT-I cells in second recipient mice were analyzed. **(B)** The expression of CD69 and CD103 by donor OT-I cells in the LP and IEL compartment of indicated second recipient mice. **(C)** Numbers of donor OT-I cells in tissues of indicated second recipient mice. **(D)** The expression of CD127 and KLRG-1 by donor OT-I cells in indicated tissues at >30 d after transfer into congenic naive second recipient mice. **(E)** Experimental design for F. 1 × 10^4 naive OT-I cells were transferred into congenic naive first recipient mice 1 d prior to i.v. infection with InlA^M *Lm*-OVA. At 5.5 dpi, effector OT-I cells were isolated from the spleen and transferred into congenic second recipient mice that were uninfected or foodborne infected with InlA^M *Lm*-OVA 5.5 d previously. 3 d after transfer, donor OT-I cells in second recipient mice were analyzed. **(F)** The expression of CD69 and CD103 by donor OT-I cells in the IEL compartment of indicated second recipient mice. **(G)** Experimental design for H. 1 × 10^4 naive OT-I cells were transferred into congenic naive first recipient mice 1 d prior to i.v. infection with InlA^M *Lm*-OVA. At 5.5 dpi, effector OT-I cells were isolated from the spleen and transferred into congenic naive second recipient mice. 6 d after transfer, second recipient mice were treated with vehicle control or FTY720 daily for 3 wk followed by analysis of donor OT-I cells. **(H)** The expression of CD69 and CD103 by donor OT-I cells in the LP and IEL compartment of indicated second recipient mice. The data in B and C are pooled from two independent experiments, *n* = 8–9 mice total. The data in D are representative of two independent experiments, *n* = 4 mice/experiment. The data in F are pooled from two independent experiments, *n* = 3–4 mice total. The data in H are pooled from two independent experiments, *n* = 5–6 mice total. The data are expressed as mean ± SEM. Unpaired *t* tests were performed (B–D, F and H). *, P ≤ 0.05; **, P ≤ 0.01; ***, P ≤ 0.001; ****, P ≤ 0.0001.

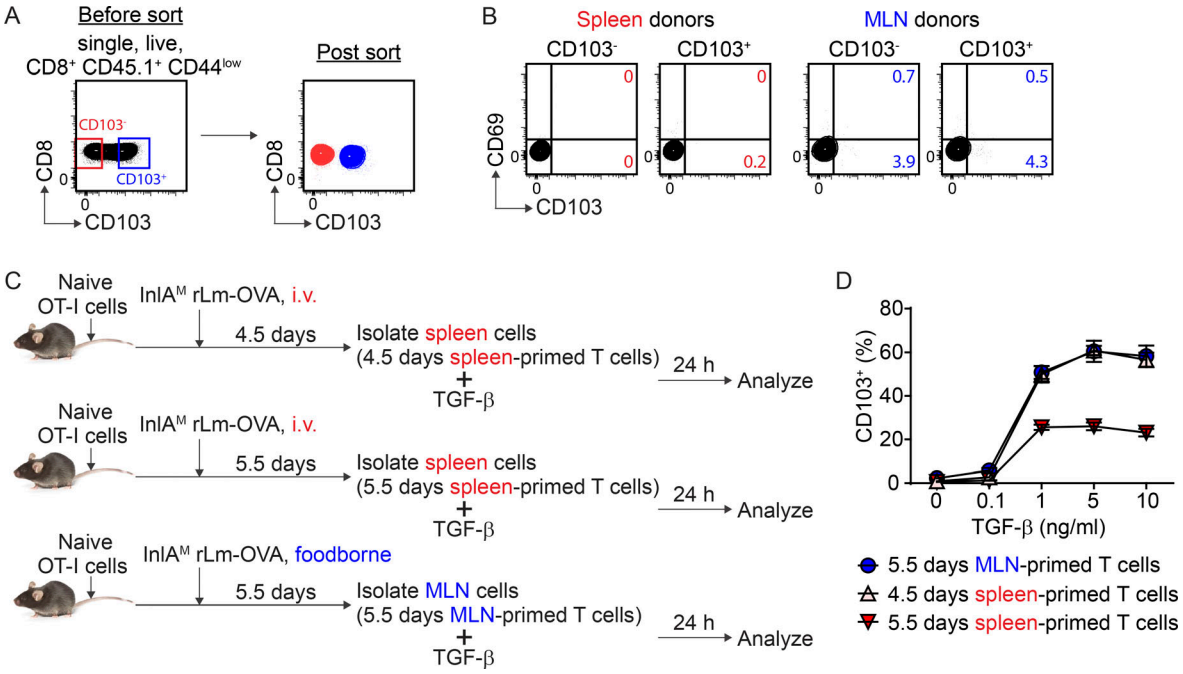

Figure S4. **The sorting strategy for CD103⁻ and CD103⁺ naive OT-I cells, the expression of CD69 and CD103 by transferred CD103⁻ and CD103⁺ naive OT-I cells after activation, and the ability to upregulate CD103 expression in response to TGF-β by Spleen and MLN donors. (A)** The gating strategy for sorting CD103⁻ and CD103⁺ naive OT-I cells. **(B)** The expression of CD69 and CD103 by spleen donors and MLN donors depicted in Fig. 3 A. **(C)** Experimental design for D. 1×10^4 naive OT-I cells were transferred into congenic naive recipient mice 1 d prior to i.v. or foodborne infection with InlA^M *Lm*-OVA. 4.5 and 5.5 d spleen-primed T cells and 5.5 d MLN-primed T cells were cultured with TGF-β in vitro for 24 h followed by flow analysis of CD103 protein expression. **(D)** The CD103 expression by 4.5 and 5.5 d spleen-primed T cells as well as 5.5 d MLN-primed T cells. The data in A are representative of four independent experiments. The data in B are from one experiment. The data in D are representative of two independent experiments and expressed as mean ± SEM, *n* = 4 mice/experiment.

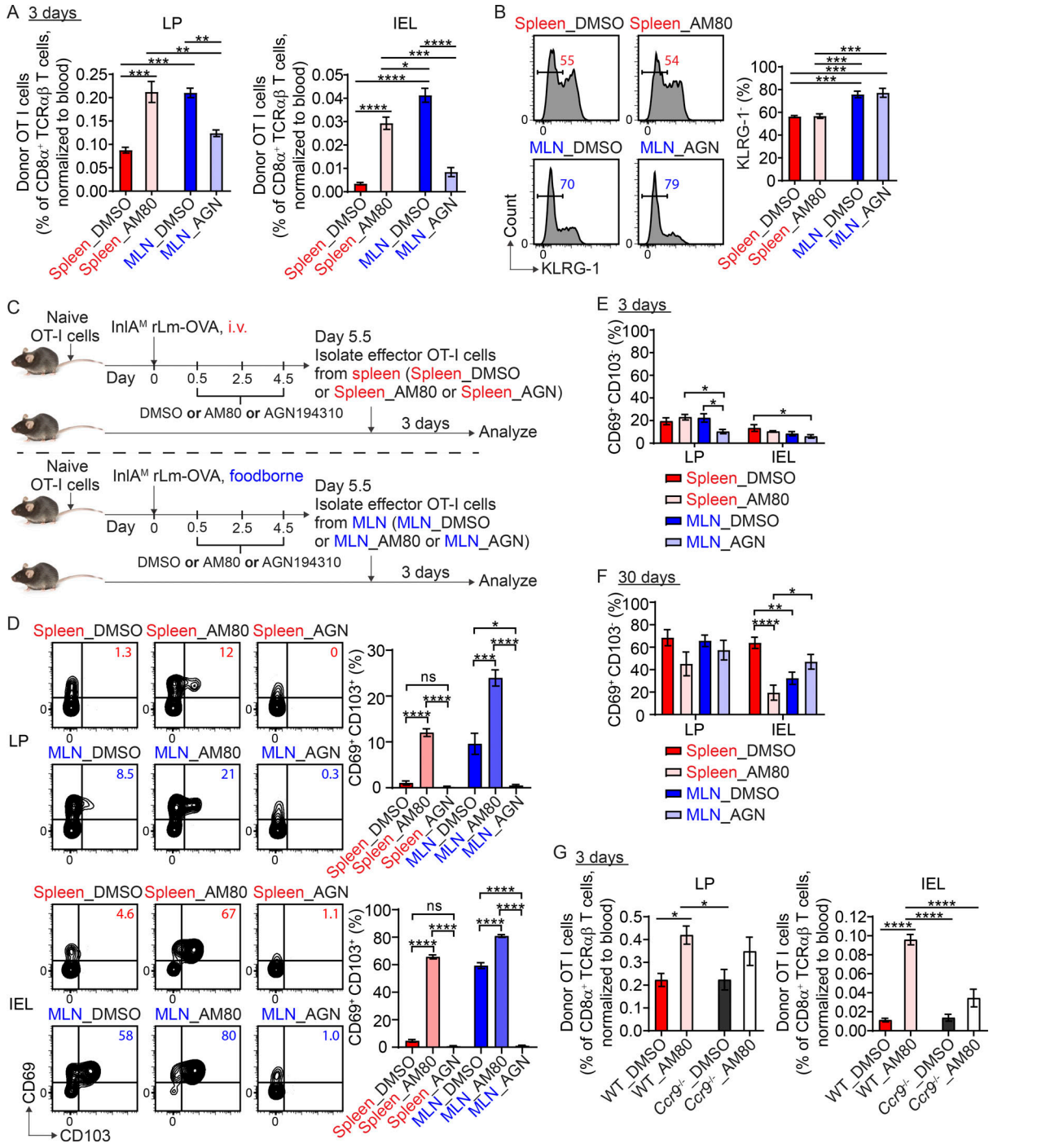

Figure S5. **The effect of RA signaling modulation on effector T cell migration to the intestine, KLRG-1 expression, and T_{RM} precursor cell differentiation. (A)** The normalized percentage of indicated donor OT-I cells in the LP and IEL compartment at 3 d after transfer. **(B)** The percentage of KLRG-1$^-$ population in indicated effector OT-I cells prior to adoptive transfer. **(C)** Experimental design for D. 1×10^4 naive OT-I cells were transferred into congenic naive first recipient mice 1 d prior to i.v. or foodborne infection with InlA^M *Lm*-OVA. Mice were treated with DMSO control, AM80, or AGN194310 at 0.5, 2.5, and 4.5 dpi. At 5.5 dpi, effector OT-I cells were sorted from the spleen of i.v.-infected or the MLN of foodborne-infected mice and transferred into congenic naive second recipient mice. 3 d after transfer, donor OT-I cells in second recipient mice were analyzed. **(D)** The expression of CD69 and CD103 by indicated donor OT-I cells in the LP and IEL compartment at 3 d after transfer. **(E)** The percentage of CD69$^+$ CD103$^-$ population in indicated donor OT-I cells in the LP and IEL compartment at 3 d after transfer. **(F)** The percentage of CD69$^+$ CD103$^-$ population in indicated donor OT-I cells in the LP and IEL compartment at 30 d after transfer. **(G)** The normalized percentage of indicated donor OT-I cells in the LP and IEL compartment at 3 d after transfer. The data in A are representative of two independent experiments, *n* = 4 mice/experiment. The data in B are pooled from three independent experiments, *n* = 5–6 mice total. The data in D are pooled from two independent experiments, *n* = 4–5 mice total. The data in E are representative of two independent experiments, *n* = 4 mice/experiment. The data in F are pooled from four independent experiments, *n* = 6–8 mice total. The data in G are representative of two independent experiments, *n* = 4 mice/experiment. The data are expressed as mean ± SEM. One-way ANOVA with Tukey's multiple comparisons tests were performed (A, B, and D–G). *, P ≤ 0.05; **, P ≤ 0.01; ***, P ≤ 0.001; ****, P ≤ 0.0001.

Provided online is Table S1, which lists differentially regulated genes between spleen-primed and MLN-primed T cells.